

# Principles and Topical Applications of $^{19}\text{F}$ NMR Spectrometry

Paul D. Stanley

Syngenta, Jealott's Hill International Research Centre, Bracknell, RG42 6ET, UK

E-mail: paul.stanley@syngenta.com

Fluorine occurs naturally in only a few organic compounds. In the chemical industry fluorine is a substituent of choice used to modify synthetic substrates in expectation of conferring beneficial physical properties. When incorporated, the spectroscopic properties of fluorine make it a useful tool to aid the structural elucidation of the derived substances. Fluorine is generally resistant to degradation and offers interesting possibilities as a probe for the determination of chemical residues and the investigation of metabolic processes. This chapter offers an overview of the ways in which the many recent advances in NMR technology can be exploited to derive useful qualitative and quantitative chemical information from fluorinated substances.

**Keywords.**  $^{19}\text{F}$  NMR Experimental procedures, Chemical shifts and coupling constants, Structure elucidation, Metabolites, Quantitative analysis, Illustrative applications of  $^{19}\text{F}$  NMR, Fluorine tags

1	Introduction	3
1.1	General Principles of NMR Spectroscopy	3
1.2	Application of NMR Spectroscopy to Chemical Structure Determination	5
1.3	NMR Experiments for Chemical Structure Confirmation	6
1.4	NMR Experiments for Chemical Structure Elucidation	7
1.5	Computational Methods	9
1.6	$^{19}\text{F}$ NMR Spectra – Chemical Shifts and Coupling Constants	11
1.7	Acquisition of $^{19}\text{F}$ NMR Spectra – Instrumental Considerations	16
1.8	Mass Spectrometry and NMR as Complementary Procedures	18
2	Topical Applications of $^{19}\text{F}$ NMR Spectrometry	20
2.1	Structure Elucidation – Tefluthrin, a Case Study	20
2.2	LC/NMR and Metabolite Identification	36
2.3	Quantitation of Metabolites	45
2.4	Solid State NMR Applications	49
2.4.1	Gels	49
2.4.2	Semi-Solids	50

2.4.3	Solids . . . . .	50
2.5	Biochemical Studies . . . . .	51
2.5.1	Labels and Tags . . . . .	51
2.5.2	Magnetic Resonance Imaging (MRI) . . . . .	52
2.5.3	Drug Design . . . . .	52
2.6	Determination Optical Purity – Fluorinated Derivatisation Reagents . . . . .	53
3	<b>Conclusions and a Prospective View . . . . .</b>	55
4	<b>Appendix . . . . .</b>	56
5	<b>References . . . . .</b>	57

### List of Abbreviations

$\delta$	dimensionless unit (chemical shift scale)
J	spin-spin coupling constant (Hz)
ppm	parts per million (chemical shift scale)
ppb	parts per billion (concentration)
APT	<i>Attached Proton Test</i>
COLOC	<i>CORrelation spectroscopy via LONG range Coupling</i>
COSY	<i>CORrelation SpectroscopY</i>
DEPT	<i>Distortionless Enhancement by Polarisation Transfer</i>
FLOCK	long range heteronuclear correlation experiment using Bird pulses
GARP	<i>Globally optimised Alternating-phase Rectanglar Pulses</i>
HETCOR	<i>HETeronuclear CORrelation</i>
HETGOESY	<i>HETeronuclear Gradient Overhauser Enhancement SpectroscopY</i>
HMBC	<i>Heteronuclear Multiple Bond Correlation</i>
HOESY	<i>Heteronuclear Overhauser Enhancement SpectroscopY</i>
HSQC	<i>Heteronuclear Single Quantum Coherence</i>
INADEQUATE	<i>Incredible Natural Abundance Double QUAntum Transfer</i>
MRI	<i>Magnetic Resonance Imaging</i>
NOESY	<i>Nuclear Overhauser Enhancement SpectroscopY</i>
ROESY	<i>Rotating frame Overhauser Enhancement SpectroscopY</i>
TOCSY	<i>TOTAL Correlation SpectroscopY</i>
WALZ	a broadband decoupling pulse sequence
WURTZ	a broadband decoupling pulse sequence

## 1 Introduction

This chapter provides an account of the overall principles of NMR spectroscopy with particular reference to the acquisition and interpretation of  $^{19}\text{F}$  NMR data. It introduces the concepts of the correct selection of instrumental parameters, NMR pulse methodologies (such as COSY), instrumentation, and the application of LC-NMR interfaces. Rather than provide a summary of numerous applications, the structural determination of a specific compound is discussed in detail so as to illustrate the importance of  $^{19}\text{F}$  as a probe and reporter of chemical structure. In many biochemical applications, a complete knowledge of the structure of metabolites is of primary importance and thus is discussed in terms of qualitative identification, quantitation, and determination of optical configuration. Attention is drawn to applications in analytical chemistry and microbiology, both discussed elsewhere in this volume, where no theoretical background is presented, and to the fact that many other industrial applications involving perfluorinated compounds are not discussed.

In this section we take a representative selection from the many experiments and tools that can be used to realise the potential of NMR as a generic tool to solve chemical structures. This account is biased by the substances handled within our laboratory and thus does not consider the large amount of work on perfluorinated materials that are important elsewhere in the chemical industry. The presence of  $^{19}\text{F}$  atoms, and fluorinated groups, in chemical structures are powerful probes of subtle structural information that can be accessed using many standard NMR methods. For complex, or unknown, substances where a result is needed against a tight deadline, computational methods may aid the process of structure elucidation.

### 1.1 General Principles of NMR Spectroscopy

Within the context of this chapter, detailed discussions of the physics of the NMR phenomenon and the ever increasing number of NMR experiments that may be applied to elicit unique pieces of structural chemical information are not appropriate. This information will be found readily in the many excellent general and specialist NMR texts available. Those currently popular amongst the chemists in our laboratory include the works by Hore [49], Sanders and Hunter [89] and the late Andy Derome [31]. The recent text by Claridge [27] promises to become the preferred general work for NMR users and practitioners alike. In reviewing this text Bladon [12] points out that the author caters for three classes of reader: (1) NMR users who have no interaction with spectrometers, (2) those who have also been trained to acquire their own data and (3) the non-specialist responsible for instrument maintenance. The identification of this last classification of user, together with hints on how to negotiate with manufacturers surely makes the book unique. This book gives a clear, readable and comprehensive introduction to NMR and is thoroughly recommended by the reviewer. It should be noted that none of these texts are specific to  $^{19}\text{F}$  NMR.

Though out of print, the books by Dungan and Van Wazer [34] and Mooney [65] are worth searching out since they deal specifically with the topic and are still widely referenced today.

The feature that is common to all NMR spectra, and that accounts for its widespread application to chemical structure determination, is that NMR spectra report substances as sets of optionally connected chemical substructures. The signals from each substructure give rise to a characteristic NMR fingerprint. These fingerprints are reproducible and generally predictable by nature. A retrospective assembly of all the identified substructures may reveal several structural alternatives. Most often, these can be discriminated by further NMR experimentation.

The following pieces of information are readily extracted from NMR spectra and are the building blocks that lead to the successful elucidation of chemical structures.

- Chemical shift ( $\delta$ ) - NMR spectroscopy differentiates between atomic nuclei in different chemical environments. Nuclei in different chemical environments have signals with different positions along the  $x$ -axis of the spectrum (chemical shift). Nuclei in similar chemical environments have similar chemical shifts. Chemical shifts are normally measured relative to a small amount of a known compound (*internal standard*) added to the test sample.
- Signal intensity - essentially, the NMR experiment is quantitative and with due care the areas of NMR signals can be measured (by electronic *integration*) to determine the relative number of nuclei giving rise to each signal. In mixtures, the ratio of peak integrals can be used to estimate molar composition; in pure materials, the same ratio can be used to propose an empirical formula.
- Spin-spin coupling ( $J$ ) - NMR signals may appear as sharp peaks or have characteristic splitting patterns that result from the magnetic interaction of one nucleus with another. Spin-spin coupling may be observed between nuclei of the same kind (e.g.  $^{19}\text{F}$ - $^{19}\text{F}$ ) and between nuclei of different kinds (e.g.  $^{19}\text{F}$ - $^1\text{H}$  or  $^{19}\text{F}$ - $^{13}\text{C}$ ). Chemically isolated nuclei have no such interactions and appear as single peaks.
- Relaxation times ( $T_1$ - $T_2$ ) - when radiofrequency energy is absorbed to generate an NMR signal it must be allowed to dissipate before further experimental data can be acquired. There are two time-dependant mechanisms by which this energy is dissipated: either to the environment ( $T_1$ ) or by interaction with local non-fluctuating magnetic fields ( $T_2$ ). Knowledge of the approximate relaxation times of different nuclei in the same sample is a key factor in achieving accurate quantitation of NMR spectra.

Most fluorinated compounds of interest to the chemist will contain  $^{19}\text{F}$ ,  $^1\text{H}$  and  $^{13}\text{C}$  atoms. The nuclear properties of these nuclides are shown in (Table 1).

At first glance, there is little to differentiate between the nuclear properties of  $^{19}\text{F}$  and  $^1\text{H}$  in terms of sensitivity and natural abundance, additionally both nuclei also have  $T_1$  relaxation times that are short enough to allow the meaningful quantitation of the signals. With modern medium-field NMR instruments, it is possible to obtain good quality  $^1\text{H}$  and  $^{19}\text{F}$  spectra on sub-milligram amounts of

**Table 1.** Nuclear properties of  $^1\text{H}$ ,  $^{13}\text{C}$  and  $^{19}\text{F}$ 

Nuclide	Nuclear spin, $I$	Relative sensitivity	Natural abundance (%)	$\nu_0$ (MHz) at 9.4 T	$\gamma$ ( $10^7 \text{ rad T}^{-1} \text{ s}^{-1}$ )
$^1\text{H}$	1/2	100	99.98	400.0	26.752
$^{13}\text{C}$	1/2	1.59	1.11	100.4	6.728
$^{19}\text{F}$	1/2	83.3	100.00	376.4	25.181

substances ( $\text{MW} < 500 \text{ Da}$ ) within a few minutes. In contrast,  $^{13}\text{C}$  nuclei have both low sensitivity and low natural abundance.  $^{13}\text{C}$  nuclei often have long  $T_1$  relaxation times that make the routine use of  $^{13}\text{C}$  spectra for quantitation difficult when small amounts of sample are available. Despite these characteristics,  $^{13}\text{C}$  spectra are key components of chemical structure elucidation. If properly equipped with a low volume NMR probe, a modern medium-field NMR instrument will deliver good quality  $^{13}\text{C}$  spectra on sub milligram amounts of substances with a molecular mass  $< 500 \text{ Da}$  in less than 1 h.

NMR spectrometers are tuned to acquire spectra from only one kind of nucleus at a time, thus when tuned for  $^{19}\text{F}$  observation only signals from  $^{19}\text{F}$  containing substances are observed.

## 1.2

### Application of NMR Spectroscopy to Chemical Structure Determination

The high sensitivity and enormous chemical shift range of  $^{19}\text{F}$  NMR nuclei make  $^{19}\text{F}$  NMR an attractive proposition. Although  $^{19}\text{F}$  NMR spectra are exceptionally selective in terms of establishing and quantifying the number of fluorinated species present, the chemical shift ranges for the different fluorinated functionalities overlap extensively. Alone, therefore,  $^{19}\text{F}$  NMR data often do not add a great deal to the process of chemical structure determination. The inclusion of fluorine substituents in substances, however, provides a powerful handle that enhances the process of structure determination through consideration of the resulting spin-spin coupling pathways established from the fluorine entities to nearby  $^1\text{H}$  and  $^{13}\text{C}$  atoms.

There are four levels of refinement for the determination of chemical structure:

- Primary chemical structure (elemental composition) is normally determined using elemental analysis or high resolution mass spectrometry (HRMS).
- Secondary chemical structure (functional groups and connectivities within the molecule) is normally determined using NMR, vibrational spectroscopy and, to a lesser extent, MS.
- Tertiary chemical structure (spatial arrangement of sub-structural motifs) is normally determined using NMR or X-ray analysis.
- Quaternary structure (existence of functional domains) is normally determined using NMR or X-ray analysis.

Although X-ray crystallography is undeniably the single method of choice for the determination of chemical structures, it is often difficult to obtain crystals suitable for X-ray analysis. The application of a combination of alternative instrumental techniques then becomes necessary. The text by Crews et al. [29] presents a logically ordered approach to the solution of the chemical structures of pure natural products by the application of multiple instrumental techniques and is to be recommended as a reference strategy document. NMR spectroscopy is probably the most vital step in the process. This is not always because it is the best, or most cost effective, technique but because of a combination of the certainty of the results, the relative ease of spectral interpretation and a familiarity with the technique on the part of most chemists. Familiarity with the technique is a powerful stimulus but it should be part of every chemist's creed to take regular "reality checks" to ensure that the analyses being performed are the most appropriate and that they really are answering the questions being posed.

Although chemical intuition is an invaluable tool routinely called upon it may, occasionally, be misleading. Knowledge of the chemical route producing the substance being investigated or an educated guess as to the metabolic process leading to expression of the substance being analysed is almost always useful, but should not be used as primary information. The real structural information is there to be had in the NMR data sets on the desk in front of you, and this should form the primary source for any structural conclusions.

### 1.3

#### **NMR Experiments for Chemical Structure Confirmation**

Modern NMR technology gives access to an enormous range of experimental methodologies that probe chemical structure and make the process of structure elucidation by this technique a truly stimulating occupation. The volume by Braun et al. [15] contains details of how to set up and measure 163 separate NMR experiments. At a practical level the volume is most useful to owners of Brüker NMR systems, but it serves as an invaluable reference text for all NMR instrument users. Details of how to set up the experiments described later may be found in this volume; users of instruments from other manufacturers (e.g. JEOL and Varian) will find similar guidance in their instrument manuals. Selecting the correct post acquisition processing needed to display the NMR spectra and massaging them to give the "best" results is an art in itself. The volume by Bigler [11] is a structured introduction to the post-acquisition processing of NMR spectra that is, again, aimed at owners of Brüker NMR systems. This is an interesting book to work through since it contains carefully selected examples of good NMR data and an academic copy of the Brüker WinNMR program so that the learning can take place away from the spectrometer. Transferring the learning experience to the instrument software of other vendors is not without problems but these are relatively minor compared to the benefits.

There are two common situations to which the tactics of organic structure determination are applied. The simplest case involves proving that the sub-

stance at hand is identical to one previously reported. The other involves establishing the structure of a completely new substance. In both cases a command of the methods for translating spectroscopic data into structures is essential, a point we will come back to later.

In our laboratory the first stage is usually to acquire a simple one-dimensional (1D) proton NMR spectrum. At first sight this spectrum will give a good idea of the complexity of the substance being investigated, the purity of the sample and give some high level pointers to the type of substance being examined (e.g. aliphatic, aromatic etc.). A particular structural isomer can often be distinguished by consideration of the patterns arising from spin-spin coupling; the presence of selected other nuclei (e.g.  $^{19}\text{F}$ ) can be inferred by the presence of spin-spin couplings not explainable by the consideration of interactions between protons alone. If the presence of  $^{19}\text{F}$  substituents is suspected, or expected, the 1D  $^{19}\text{F}$  spectrum yields crude structural information about the chemical types of fluorine present and, more importantly, a sensitive double-check on the purity of the sample with respect to other fluorinated materials.

For the purposes of proving that the substance being investigated is identical to one previously reported the chase usually stops here. If, however, the structure of the analyte is unknown, or if confirmation of a previously reported structure is required, this is the starting point for a more detailed study. Acquisition of 1D  $^{13}\text{C}$  and DEPT [9] or APT [78] will determine the number of carbon atoms present and label each in terms of the number of protons attached. In conjunction with the  $^1\text{H}$  and  $^{19}\text{F}$  spectra a list of proposed substructures can be constructed. On the basis of an empirical formula deduced from the molecular weight of the substance from MS, a series of two-dimensional structures can be written.

## 1.4

### NMR Experiments for Chemical Structure Elucidation

Depending on the apparent complexity of the substance, a range of 1D and two-dimensional (2D) NMR experiments can be planned that will experimentally verify or deny the existence of the connectivities required by the proposed structures. For less complex molecules 1D NMR experiments such as homonuclear decoupling (probing  $^1\text{H}$ - $^1\text{H}$  or  $^{19}\text{F}$ - $^{19}\text{F}$  interaction) and heteronuclear decoupling (probing  $^1\text{H}$ - $^{19}\text{F}$ ,  $^1\text{H}$ - $^{13}\text{C}$  or  $^{19}\text{F}$ - $^{13}\text{C}$  interaction) experiments are often sufficient to establish the chemical substructures actually present. In the case of more complex substances 2D NMR methods such as COSY [5] (probing geminal and vicinal  $^1\text{H}$ - $^1\text{H}$  interactions) or TOCSY [16] (correlating all protons in a particular substructure) are usually applied. It should be noted that complexity is not always a function of molecular size; the spectra of small molecules are often sufficiently overlapped to preclude the use of spin-decoupling experiments. In principle, these 2D methods display every spin-spin coupling present in the molecule, rather than establishing them one at a time using spin-decoupling experiments – the habit of not using 2D methods for small molecules stems from the long time (typically several hours) required to set up, collect and process the 2D data sets. The introduction of gradient selected versions of COSY [51] and

TOCSY [51] experiments, together with the increased stability of modern NMR instruments, removes this barrier since the 2D data can now be collected in tens of minutes.

Correlations between different types of nuclei (e.g.  $^1\text{H}$ - $^{19}\text{F}$  or  $^1\text{H}$ - $^{13}\text{C}$ ) are readily established using HETCOR [42] (one bond correlations) or COLOC [58]/FLOCK [20] (long-range correlations) experiments. These spectra can take many hours to acquire, especially if limited amounts of material are available. The introduction of inverse geometry NMR probes has increased the sensitivity of the complementary proton detected experiments HSQC [13] (one bond correlations) and HMBC [17] (long range correlations) to such an extent that the direct observation experiments are falling from popular usage. For the analysis of samples, where a reasonable amount of material is available, the gradient selected versions of HSQC [57] and HMBC [7] can often cut the acquisition time of the spectra by a factor of four. The edited gradient selected HSQC [77] experiment is the equivalent of heteronuclear correlation with signal of the low frequency nuclei being edited in DEPT fashion with “even” and “odd” multiplicity carbons being separated by the phase of the signal in the 2D display. Since this experiment also correlates carbon and proton chemical shifts, inspection of the proton spectrum usually removes the uncertainty as to whether the “even” multiplicity signals are methyl or methine carbons.

In practice, unless there are unusual combinations of chemical shifts present, heteronuclear correlation experiments often do not offer useful information with reference to chemical structure determination. These spectra are, however, an indispensable part of the inevitable process of the complete retrospective unambiguous assignment of the spectra.

To establish the basic stereochemistry of molecules (e.g. the *E-Z* configurations of alkenes) the nuclear Overhauser (NOE) effect can be profitably applied. NOE depends on the dipolar relaxation of one nucleus by another. The effect is proportional to the inverse sixth power of the distance between the participating nuclei and is thus sensitive to conformational changes. There are NMR experiments designed for either homonuclear or heteronuclear applications. The basic 1D NOE difference experiment [72] collects a spectrum with external radio frequency irradiation at the peak of interest followed by a spectrum without irradiation. When these spectra are subtracted the difference signals can be correlated with proximity. 2D versions of this experiment, NOESY [73] and its gradient selected version [107], are often used to study larger molecules; it is an essential method for determining the peptide conformation (tertiary structure) of proteins. NOESY cross peaks may “vanish” for molecules with molar masses in the range 1000–3000 since the sign of the NOE effect changes sign depending upon the molecular correlation time. The NOE is always positive under the spin-lock conditions that are used in the ROESY [14] experiment. Without special spin-lock conditions [52, 53] ROESY experiments may also show TOCSY correlations that may lead to confusion.

Whereas most of the experiments mentioned above appear to focus on  $^1\text{H}$  and  $^{13}\text{C}$  NMR it should be remembered that, when  $^{19}\text{F}$  is incorporated into the chemical structure, its interaction with other nuclei through spin-spin couplings is usually far more useful as structural handles than simply observing

the  $^{19}\text{F}$  chemical shift. The clean baselines typical of  $^{19}\text{F}$  spectra often make it the nucleus of choice for the determination of the proximity relationships which lead to the successful determination of stereochemistry and 3D structures.

So it seems that the collection of a carefully selected range of NMR spectra from a sample will yield information that should make it possible to assemble a list of candidate chemical structures consistent with the observed data that can be refined to a single structural entity by further experimentation. Whilst this is undeniably true, the process is far from easy. When results are required against a short deadline it may be appropriate to seek assistance from computational aids.

## 1.5

### Computational Methods

The application to the treatment of spectroscopic data using computational methods is presently not well developed. The demands placed by the new areas of chemistry, such as solid phase synthesis and combinatorial chemistry, that have the potential to produce many thousands of samples with apparent ease have resulted in a resurgence in interest in the topic of  $^1\text{H}$  NMR spectrum prediction and appropriate display software [1]. The prediction of  $^1\text{H}$  NMR spectra is fraught with difficulties due to the unpredictable effects caused by through-space effects, changes in NMR solvent, etc. These effects are not so important with respect to  $^{19}\text{F}$  and  $^{13}\text{C}$  spectra, due to the wide chemical shift ranges involved, and it is possible to predict the spectra of these nuclei with a good degree of precision. The computer software necessary to do these calculations is available commercially [3, 24]. The products from ACD and Chemical Concepts (SpecInfo) are based on enhanced applications of the sub-structural coding routine devised by Bremser [18]. Using this scheme, each atom (node) in the molecule is assigned a code based upon its chemical environment, described in terms of the number of bonded atoms together with their bonding scheme; it is extended to consider atoms up to four chemical bonds away. The extent of each code was determined by the computer word-length available at the time. A peculiar limitation of this approach is exemplified with reference to aromatic materials, whereby the nature of a substituent *para* to any particular node is not recognized. Each node is then assigned a chemical shift during spectrum assignment, the resulting correspondences being contained in an inverted database. When used to predict the spectrum of a compound not exemplified in the database, the program disassembles the novel structure into sub-structural units (the nodes) and seeks matches in the database. Exact node for node matches are therefore reported with high confidence and values for non-exact matches with a lower confidence. Whilst originating in the prediction of  $^{13}\text{C}$  NMR data, both ACD and SpecInfo offer  $^{19}\text{F}$  predictions based upon large authenticated databases. ACD and SpecInfo quote access to 15,000 and 23,500 records respectively. As well as prediction of the spectra of novel substances, both programs offer traditional chemical shift line searches to identify substances or sub-structures with similar chemical shifts and full sub-structural database searching to access the complementary data stored along with the

chemical shift values. These typically include coupling constant information, experimental conditions and literature references. Both these programs are remarkable in as much as they accurately predict the spectra of substances that have been suggested by the analyst, who then uses experience to judge the goodness of fit between the experimental and the predicted data.

A more attractive option, however, is to allow the spectral data to speak for itself. This proposal is not so wild as it may seem. There are several prototype programs available commercially that aim to apply logic to the assembly of spectroscopically identifiable substructures. With the present level of development, each of the software toolkits described below produces creditable results under idealized conditions. In our laboratory the quality of data we are able to generate routinely is often not of sufficient quality to guarantee success.

Once in possession of a working empirical formula the Molgen [10] program will generate all chemical structures consistent with the empirical formula. The enormous numbers of proposed structures are constrained using a combination of  $^{13}\text{C}$  multiplicity and a good list – bad list principle. When the list of candidates has been reduced to a manageable number (say less than 200) the structures can be imported directly into SpecInfo; the SpecInfo program automatically predicts the  $^{13}\text{C}$  spectrum of each structure and presents a list of goodness of fit with the experimental data. Understanding the principle of good – bad lists is key to succeeding with this suite of programs. Pretsch's paper [91] offers an authoritative summary of the strategy of good list – bad list formulation.

There are commercial programs that go some way towards offering a fully automatic interpretation of spectroscopic data, and the products from ACD [2], Spectrum Research [99] and ScienceSoft [92] are worthy of note. ACD-Structure Elucidator allows automatic or manual import of spectral data from other ACD software products. At present only 1D NMR data (plus IR and MS data) can be used; the 2D NMR module is presently in beta testing. The experimental data is subjected to a sub-spectrum search in the main ACD prediction database followed by a structure generation stage based on overlapping fragments by their common atoms, a process which does not require knowledge of the molecular formula. Alternatively, a unique "spectrum filtration" procedure based on spectral features can be used to constrain the list of possible structures. The generated structures are then presented in order of goodness of fit with the data. This program works well with structures that have partial or close precedents in the main ACD prediction database.

NMR-SAMS (formerly CISOC-SES) from Spectrum Research was developed by Yuan et al. [80, 81] and utilizes NMR spectra prepared for analysis by the corresponding SpecMan program. Data from a wide range of 1D and 2D NMR experiments together with molecular formula information and structure fragment information from UV and IR methods generate structures compatible with the spectral data. The program automatically generates fixed bonds and "building blocks" using COSY,  $^{13}\text{C}$  and DEPT – APT information. The program proposes unique structures when given substantial data and partial structures when given sparse data. Since this program does not consider existing information, it has the potential to solve unprecedented chemical structures. In our hands the program performed well so long as the data was of high quality, but

was unforgiving when expected correlations were absent due to poor sensitivity etc.

ScienceSoft's NMRAnalyst is also available as FRED from Varian Inc. The package automates the interpretation of 2D NMR data. At inception the program dealt only with INADEQUATE ( $^{13}\text{C}$ - $^{13}\text{C}$  COSY) data. This NMR experiment is very insensitive and the first stage is to use novel mathematical procedures (Full Reduction of Entire Data-sets) to determine the true  $^{13}\text{C}$ - $^{13}\text{C}$  COSY correlations present in the spectrum, thus establishing the carbon skeleton. AssembleIt is the NMRAnalyst extension module for correlating the information extracted from different spectrum types. Currently, AssembleIt supports the challenging combination of short-range and long-range heteronuclear, DEPT, and 2D INADEQUATE information to derive molecular carbon skeletons. It is planned to extend AssembleIt for the complete structure elucidation of unknown compounds and for the 3D-structure determination of proteins and other bio-molecules.

In this section we have mentioned some of the experiments and tools that can be used to realise the potential of NMR as a generic tool to solve chemical structures. The presence of  $^{19}\text{F}$  atoms, and fluorinated groups, in chemical structures are powerful probes of subtle structural information that can be accessed using many standard NMR methods. For complex, or unknown, substances where a result is needed against a tight deadline, computational methods may aid the process of structure elucidation.

## 1.6

### $^{19}\text{F}$ NMR Spectra – Chemical Shifts and Coupling Constants

As indicated above,  $^{19}\text{F}$  nuclei have favourable NMR properties and since fluorine-containing substances are important industrially,  $^{19}\text{F}$  NMR has been actively studied since the discovery of the NMR experiment. Consequently, there are many thousands of literature references detailing the applications of  $^{19}\text{F}$  NMR to structural chemistry problems that span more than 40 years of industrial and academic research. Vast compilations of experimental data have been reported in the series *Annual Reports on NMR Spectroscopy* [66, 55, 56, 39, 21, 111, 112] and *Progress in NMR Spectroscopy* [35, 36] but many of the substances reported in these references are highly fluorinated and, as such, are not relevant to this chapter. Since these represent an enormous amount of information spread across several volumes these references are not convenient to use but, undeniably, include some data not exemplified in the databases supporting the  $^{19}\text{F}$  spectrum prediction approach described above. An additional complication with this literature is that it contains  $^{19}\text{F}$  chemical shifts reported using several different NMR chemical shift conventions, the relevance of which is discussed later. The only convenient way to access more recent data is to use conventional literature searching methods in the primary journals. The many journals dedicated to NMR techniques generally focus upon details of new applications for  $^{19}\text{F}$  NMR whereas the chemical literature is relied upon to report spectroscopic properties of new fluorinated substances. Everett [38] has produced the most recent authoritative review covering the NMR spectrometry of

**Table 2.** Chemical shifts of alternative reference compounds based on  $\text{CCl}_3\text{F} = \delta$  0.00

Substance	Chemical shift ( $\delta$ )
Benzenesulfonyl fluoride – $\text{C}_6\text{H}_5\text{SO}_2\text{F}$	+ 65.50
Trichlorofluoromethane – $\text{CCl}_3\text{F}$	0.00
Dichlorodifluoromethane – $\text{CCl}_2\text{F}_2$	- 6.90
$\alpha, \alpha, \alpha$ -Trifluorotoluene – $\text{C}_6\text{H}_5\text{CF}_3$	-63.90
1,2-Difluorotetrachloroethane – $\text{CCl}_2\text{FCCl}_2\text{F}$	-67.30
Methyl trifluoroacetate – $\text{CF}_3\text{CO}_2\text{CH}_3$	-74.21
Trifluoroacetic acid – $\text{CF}_3\text{CO}_2\text{H}$	-78.50
1,1,1-Trichlorotrifluoroethane – $\text{CCl}_3\text{CF}_3$	-82.20
Hexafluoroacetone – $\text{CF}_3\text{COCF}_3^a$	-84.60
Fluorobenzene – $\text{C}_6\text{H}_5\text{F}$	-113.15
1,4-Difluorobenzene – $\text{FC}_6\text{H}_4\text{F}$	-120.00
Hexafluorobenzene – $\text{C}_6\text{F}_6$	-162.90

Chemical shifts measured in non-polar solvent.

<sup>a</sup> Note that, in aqueous solution, hexafluoroacetone exists as the hydrate  $(\text{CF}_3\text{C}(\text{OH})_2\text{CF}_3)$  with a chemical shift of  $\delta$  -92.80.

organofluorine compounds. In this review, the author discusses and references sample spectroscopic data from a carefully selected range of fluorinated substances that are likely to be of interest to organic chemists. The references are backed up with reproductions of many high quality <sup>19</sup>F spectra that illustrate the, sometimes unusual, appearance of <sup>19</sup>F-<sup>19</sup>F and <sup>19</sup>F-<sup>1</sup>H spin-spin coupled systems.

The internationally agreed internal reference substance for <sup>19</sup>F NMR is trichlorofluoromethane ( $\text{CCl}_3\text{F}$ ) and a representative selection of some of the alternative substances used in the past are shown in Table 2, in which their chemical shifts are shown referenced to ( $\text{CCl}_3\text{F}$ ).

*External referencing* is occasionally reported. This is achieved by either insertion of a sealed sample of the referencing substance into the analyte prior to spectroscopic analysis or by simply assigning the reference position to a data point that represents the chemical shift of the standard as determined experimentally. This mode of referencing leads to significant errors in chemical shift measurement, particularly if the external reference substance is dissolved in a different solvent to the analyte. Solvent change induced shifts of >5 ppm are not unusual.

<sup>19</sup>F NMR data should be acquired and reported using the guidelines laid down by the International Union for Pure and Applied Chemistry (IUPAC) as shown in Appendix 1. The IUPAC guidelines ensure that signals for all commonly occurring organofluorine substances will be properly observed. However, these conditions demand a very wide spectrometer sweep width that may result in a problem with processing the data and that will necessitate the re-running of the spectrum over selected narrower areas if spin-spin couplings are to be measured with any precision.

When  $\text{CCl}_3\text{F}$  is used as an internal reference, the majority of commonly occurring organofluorine residues (with the exception of  $\text{RCOF}$  and  $\text{RSO}_2\text{F}$ ) have

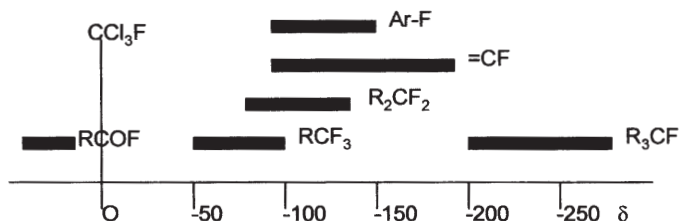


**Fig. 1.** Chemical shift ranges of commonly occurring fluorine containing organic groups

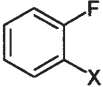
negative chemical shifts (i.e. they appear to the right of the  $\text{CCl}_3\text{F}$  signal). In contrast to  $^1\text{H}$  NMR spectra, in which the signals from protons bonded to  $sp^3$  and  $sp^2$  carbons are distinctly separated, the chemical shift ranges for fluorine atoms bonded to  $sp^3$  and  $sp^2$  carbons overlap extensively. Figure 1 illustrates the likely shift ranges for commonly occurring fluorine containing organic groups.

The theoretical background that is necessary to explain the origin of  $^{19}\text{F}$  chemical shifts is currently incomplete. The wide chemical shift range for commonly occurring  $^{19}\text{F}$  functionalities arises from large paramagnetic contributions in the shielding constant. These contributions arise from the low-lying orbitals in  $^{19}\text{F}$  atoms, which are subjected to electronic excitations by the external magnetic field  $B_0$  of the NMR spectrometer, and result in variable down-field shifts for the NMR signal from  $^{19}\text{F}$  nuclei. In the case of  $^{19}\text{F}$  nuclei, diamagnetic contributions to the screening constant are very small (1%) and the effects of neighbouring groups are essentially negligible. For example, when fluorine is bonded to a  $sp^3$  hybridised carbon atom, a definite trend in chemical shift exists within the series  $\text{R}-\text{CF}_3$ ,  $\text{R}_2\text{CF}_2$ ,  $\text{R}_3\text{CF}$ . The signals from  $\text{R}_3\text{CF}$  groups appear at highest field with respect to the others. This is accounted for by the fact that the increasing substitution of the  $sp^3$  carbon by fluorine reduces the ionic character of the resulting C–F bonds. Owing to reduced symmetry, the paramagnetic contribution to the shielding constant becomes larger, resulting in increasing downfield shifts for the signals from  $\text{R}_2\text{CF}_2$  and  $\text{R}-\text{CF}_3$  groups respectively.

The chemical shifts of  $^{19}\text{F}$  resonances may also be affected by steric (van der Waals) interactions. This can be illustrated with reference to the  $^{19}\text{F}$  chemical shifts of the series of *ortho* substituted fluorobenzenes shown in Table 3, in which the  $^{19}\text{F}$  resonances are progressively deshielded by their interaction with groups of increasing bulk.

In addition to large chemical shift ranges,  $^{19}\text{F}$  NMR spectra are also characterized by relatively large values for spin-spin coupling interactions between

**Table 3.** Chemical shifts of *ortho* substituted fluorobenzenes

	X	Chemical shift ( $\delta$ )
	F	-132
	Cl	-109
	Br	-100
	I	-87

**Table 4.** Geminal, vicinal and longer-range  $^{19}\text{F}/^{19}\text{F}$  and  $^{19}\text{F}/^1\text{H}$  coupling constants (Hz)

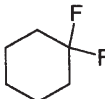
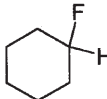
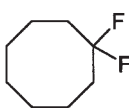
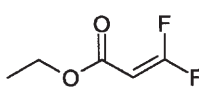
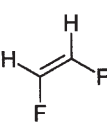
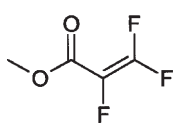
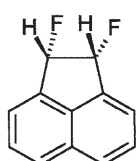
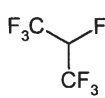
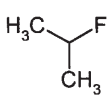
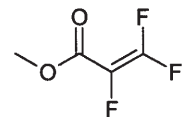
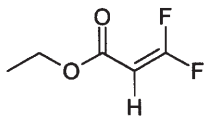
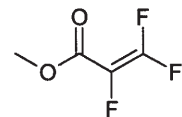
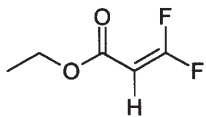
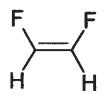
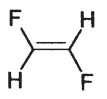
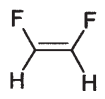
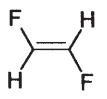
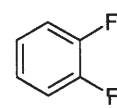
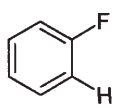
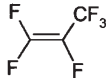
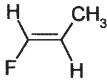
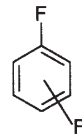
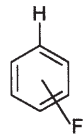
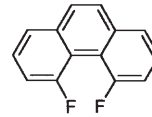
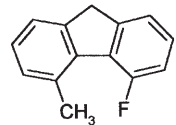
		$\text{CH}_3\text{CH}_2\text{F}$	
	$^2J_{\text{FF}}$ 157		$^2J_{\text{FH}}$ 49
	$^2J_{\text{FF}}$ 244		$^2J_{\text{FH}}$ 49
	$^2J_{\text{FF}}$ 297		$^2J_{\text{FH}}$ 85
	$^2J_{\text{FF}}$ 16		$^2J_{\text{FH}}$ 73
	$^2J_{\text{FF}}$ 26		$^2J_{\text{FH}}$ 55
$\text{CF}_3\text{CF}_2\text{CF}_2\text{CO}_2\text{H}$	$^3J_{\text{FF}}$ 1.4	$\text{CH}_3\text{CH}_2\text{F}$	$^3J_{\text{FH}}$ 27
	$^3J_{\text{FF}}$ 4		$^3J_{\text{FH}}$ 20
	$^3J_{\text{FF}}$ 111 ( <i>trans</i> )		$^3J_{\text{FH}}$ 22 ( <i>trans</i> )
	$^3J_{\text{FF}}$ 35 ( <i>cis</i> )		$^3J_{\text{FH}}$ 85 ( <i>cis</i> )
	$^3J_{\text{FF}}$ 19		$^3J_{\text{FF}}$ 125
	$^3J_{\text{FH}}$ 20		$^3J_{\text{FH}}$ 4
	$^3J_{\text{FF}}$ 20		$^3J_{\text{FH}}$ 6–10

Table 4 (continued)

$\text{CF}_3\text{CF}_2\text{CF}_2\text{CO}_2\text{H}$	$^4J_{\text{FF}}$ 10		
	$^4J_{\text{FF}}$ ( <i>cis</i> ) 22 $^4J_{\text{FF}}$ ( <i>trans</i> ) 8 $^3J_{\text{FF}}$ 13		$^4J_{\text{FH}}$ 3
	$^4J_{\text{FF}}$ ( <i>meta</i> ) $\pm 20$ $^5J_{\text{FF}}$ 5–18		$^4J_{\text{FH}}$ ( <i>meta</i> ) 6–8 $^5J_{\text{FH}}$ 2
“through space” interactions			
	170		8

both  $^{19}\text{F}$ - $^{19}\text{F}$  and  $^{19}\text{F}$ - $^1\text{H}$  nuclei. This often leads to the production of very complex signals at each chemical shift. Fortunately the relative magnitude of  $^{19}\text{F}$ - $^{19}\text{F}$  and  $^{19}\text{F}$ - $^1\text{H}$  spin-spin coupling constants compared with the potentially large chemical shift differences between coupling  $^{19}\text{F}$  nuclei leads to the situation whereby many  $^{19}\text{F}$  spectra can be interpreted using first-order rules. Table 4 gives a brief survey of geminal (2-bond), vicinal (3-bond) and longer-range spin-spin coupling constants. In this table, the signs of the spin-spin coupling constants are not given; the absence of this information should not be important except in the case of 1,3-difluorobenzenes where the experimental values of the 4-bond  $^{19}\text{F}$ - $^{19}\text{F}$  coupling constant lie in the range  $\pm 20$  Hz, and they can be, and often are, 0 Hz.

The rules used for proton spin-spin coupling cannot always be used to interpret the corresponding fluorine interactions. Spin-spin couplings are generally regarded as being transmitted through chemical bonds. In the case of fluorine nuclei, there is evidence that spin-spin couplings from fluorine nuclei may also be transmitted by a direct mechanism *through space*. The *through space* effect is envisaged as originating from scalar spin-spin coupling through non-bonding orbital overlap rather than from dipolar interactions. These long-range couplings can be detected through more than five bonds in fluorine, proton and carbon NMR spectra and provide insights into conformational preferences [106].

## 1.7

### Acquisition $^{19}\text{F}$ NMR Spectra – Instrumental Considerations

NMR spectra can be acquired using either continuous wave (CW) or pulsed Fourier transform (PFT) NMR spectrometers. Although basically quite similar, they differ in the power and time dependence of the spectrum exciting RF wave and the mode of signal acquisition. CW instruments record a classical absorption signal whereas the PFT instruments use a digital process to acquire an interferogram, known as a free induction decay (FID), by means of an analog-to-digital converter and a computer. Subsequent Fourier transformation of this time-domain data yields the frequency domain spectrum as acquired under CW conditions. The immediate advantages of PFT instruments are that they allow the fast acquisition of many spectra which are co-added, before processing, to increase the signal-noise ratio of the measured spectrum and the application of the multiple pulse experiments that are the basis of modern structure elucidation methods. Since their introduction, PFT spectrometers have become the instrument of choice for the observation of all NMR spectra. The early work reports spectrum characteristics obtained from continuous wave instruments at low field and is limited to the measurement of chemical shifts and spin-spin coupling constants. Due to the high sensitivity and wide spectral range of  $^{19}\text{F}$  nuclei, there were few technical problems in amassing the enormous libraries of data referred to in Sect. 1.5.

Modern pulsed Fourier transform NMR spectrometers have multiple radio-frequency channels to allow observation, decoupling and access to multi-pulse NMR experiments. There are no NMR experiments commonly used that require more than four radio frequency channels. The major manufacturers often offer a choice between “routine” and “research” grade PFT instruments; often the differentiation between the “routine” and “research” grade instruments lies in the system’s potential for expansion. That is, most “routine” instruments have a fixed design that means it is not possible to add extra capability if the user’s needs change after purchase. In practice, “routine” instruments allow access to all the NMR experiments needed for the structural investigation of organic materials. The choice of magnet is fundamental in establishing the final cost of the NMR spectrometer. Whilst “routine” systems are normally offered with magnets delivering proton frequencies of 200–500 MHz, “research” systems are available with magnets delivering proton frequencies 200–900 MHz. The benefits of aspiring to the highest field magnet affordable are due to the accompanying higher sensitivity and spectral dispersion. Except in special cases, where the need for sensitivity is paramount (e.g. LC-NMR) or when extra spectrum dispersion is required to address particular classes of substances (e.g. carbohydrates), the need to acquire a system with a magnet delivering proton frequencies of above 500 MHz is not well developed for most problems in organic chemistry. In the case of  $^{19}\text{F}$  NMR, 400-MHz systems are normally adequate in terms of sensitivity and avoid operational problems that may occur from the extremely wide sweep widths encountered in  $^{19}\text{F}$  NMR spectra.

In organic chemistry laboratories, spectrometers are normally configured to handle samples presented to the instrument in the “solution state”. In this con-

figuration there are a bewildering set of alternatives of NMR probes to select from. First, there is the choice between probes designed for conventional NMR tubes and flow-probes. Driven by experiments using LC-NMR and the need for the high throughput analysis of combinatorial chemistry samples, flow-probes are becoming a more popular choice for routine use due to their mass efficiency, measured in terms of ability to detect low masses of analyte. LC-NMR probes are optimised for proton observation, but some early designs of flow-probes allow the proton channel to be retuned for  $^{19}\text{F}$  observation.

For conventional probes, no single design is universal and each configuration will find a place in a laboratory working in a specialist area. In most cases, more than one probe will be specified with each instrument to cover efficiently the complete range of experiments needed to effect structure elucidation by NMR. Except for specialist laboratories, the purchase of a dedicated  $^{19}\text{F}$  probe is often regarded as a luxury, but many chemists still require access to  $^{19}\text{F}$  NMR data. The usual compromise is to select a “tuneable” probe that allows the observation of  $^{19}\text{F}$  NMR spectra. For tuneable probes, the choice will be between a manually tuned probe with a fixed proton channel and a tuneable channel that covers a range of other lower frequency nuclei (typically  $^{31}\text{P}$ – $^{15}\text{N}$ ) or a probe with three or four fixed frequencies (e.g.  $^1\text{H}$ ,  $^{19}\text{F}$ ,  $^{31}\text{P}$  and  $^{13}\text{C}$ ). The latter is a popular choice since it covers the nuclei of most interest to organic chemists and removes the need to re-tune the probe between samples. In practice, these probes have limitations that need to be considered. In general, they will be calibrated using test-samples dissolved in a particular solvent (say  $\text{CDCl}_3$ ). Changing from one solvent to another (e.g. from  $\text{CDCl}_3$  to  $\text{D}_2\text{O}$ ) will introduce a change in performance of the probe, both in terms of overall sensitivity and a change in pulse duration that will, particularly, affect the appearance of DEPT spectra. One “work-around” is to generate calibration sets for each solvent likely to be used and implement them as part of the set-up for each new experiment, but this represents effort arguably best expended elsewhere. These effects become more dramatic as the field strength increases; at 300 MHz Varian offer an ABT (Always Beautifully Tuned) probe which is not sensitive to solvent changes. Above 400 MHz the effects are real and alternatives to get around this problem are offered in the form of the JEOL auto-tuneable probe and the PulseTune accessory from the Nalorac Corporation. Under computer control, each of these devices will tune and match the probe for each sample. As with flow probes,  $^{19}\text{F}$  is detected by retuning the proton channel.

Tuneable probes are also likely to deliver a less than perfect spectrum baseline due to signals detected from the fluorinated components and glues used in the construction of the probe. These materials are used to ensure an acceptable spectrum baseline in the proton NMR spectra. Although the  $^{19}\text{F}$  spectrum baseline artefact signal is not normally intrusive when normal concentrations of analyte are used, it does assume importance when the spectrum is composed of a collection of very small signals. Even for normal strength samples, it is desirable to remove the baseline artefact for other than cosmetic purposes; subsequent spectrum processing (e.g. phase correction, peak listing etc.) is far more controllable when the spectrum baseline is flat. The baseline artefact can be removed effectively using post-acquisition linear prediction routines [84] nor-

mally found in current instrument software; if these are not available, advanced baseline correction software (e.g. as found in ACD-NMR Processor) is worth considering.

So far, we have a PFT spectrometer that acquires  $^{19}\text{F}$  NMR data comparable to that obtainable on a CW instrument, i.e. it allows recording of  $^{19}\text{F}$  NMR chemical shifts and the measurement of spin-spin coupling constants. Without a spectrometer deliberately configured to observe  $^{19}\text{F}$  spectra, access to more complex NMR experiments is not always facile.

Whereas spin-decoupling in proton NMR and the broadband decoupling of protons during the acquisition of  $^{13}\text{C}$  spectra ( $\{^1\text{H}\}^{13}\text{C}$ ) are commonplace, the decoupling of  $^{19}\text{F}$  nuclei is problematic due to the very wide spectral width of  $^{19}\text{F}$  spectra. Traditional methods of broadband decoupling (e.g. WALZ, GARP) do not work well because their limited bandwidths mean that high power levels need to be employed to cover wide spectral regions.

Recent advances in adiabatic decoupling schemes (e.g. WURST) make it possible to generate very wide bandwidths with minimum power requirements. A recent article [23] describes the experimental considerations necessary to perform either proton decoupled fluorine ( $\{^1\text{H}\}^{19}\text{F}$ ) or fluorine decoupled proton ( $\{^{19}\text{F}\}^1\text{H}$ ) experiments on Varian Inova Spectrometers configured for specialist (e.g. dedicated H-F probe with a third broadband channel) or general (e.g. AutoSwitchable probe with a single high-band amplifier) use. When the instrument is configured to perform these experiments the acquisition of 2D  $^{13}\text{C}$ - $^{19}\text{F}$  correlation experiments is possible. In a subsequent article [105] the implementation of a variety of  $^{19}\text{F}$ - $^1\text{H}$  double resonance experiments is discussed. Due to the wide variation in proton-fluorine spin-spin coupling constants,  $^1\text{H}$ - $^{19}\text{F}$  ge-COSY is an experiment that is ideal for proton-fluorine correlation since no fixed delays, incorporated to optimise for a particular value of spin-spin coupling, are required. 1D  $^{19}\text{F}$  filtered HMQC, HMQC-TOCSY and HMQC-NOESY are also described.

## 1.8

### Mass Spectrometry and NMR as Complementary Procedures

In laboratories that have access to both mass spectrometers and NMR spectrometers there is normally little, or no, conflict regarding the application of each kind of instrument. Whereas MS gives primitive structural information that is ideal for confirmatory purposes, NMR gives precise structural information that is normally reserved for chemical structure determination. In special areas (such as protein sequencing) MS may be used to derive structural chemical information, but this should not be confused with the total structure determination of the functional structure of proteins as determined by X-ray or NMR. MS is a sublimely sensitive technique often requiring only picomoles of material; at a conservative estimate, MS is two orders of magnitude more sensitive than NMR, which is compromised when a sample of much less than a microgram of substance is to be analysed. In special applications (e.g.  $^{19}\text{F}$  NMR analysis of fluorinated metabolites) NMR can almost compete on sensitivity

grounds with MS and, because of the ease of sample preparation and the added selectivity conferred by wide spectral ranges, often becomes the analytical method of choice.

To obtain MS data from a substance it must first be made to ionise and a portfolio of different methods are required to cater for the diversity of substances commonly analysed. Because of the small mass requirements for MS analysis it is often used in conjunction with a separation procedure such as gas chromatography (GC), liquid chromatography (LC) or capillary electrophoresis (CE). The text by Chapman [22] gives an up-to-date introduction to the topic of MS ionisation methods and interfaces. Presently, the major applications of MS focus on the qualitative confirmation of chemical structure with reference to a known (or proposed) material and the quantitative determinations of specific analytes using a combination of chromatography followed by MS. Presently, LC-MS is arguably the most widely used mass spectrometric technique in the areas of metabolite identification and quantitation. The volume by Willoughby et al. [109] gives an overview of the factors that determine the establishment and use of LC-MS technology in the modern laboratory.

Although NMR is not a sensitive technique, it is non-destructive and does not consume or alter the sample. It is not regarded as a selective technique in conventional terms since it reports the presence of each substance equally, without the bias inherent to MS techniques that highlight the different ionisation characteristics of each substance present. When a sample is presented for NMR analysis and the instrument is tuned to observe (say)  $^{19}\text{F}$  nuclei, every fluorinated species present will give a signal (or set of signals) characteristic of its chemical structure. Since  $^{19}\text{F}$  is a relatively rare substituent in synthetic organic molecules, the huge chemical shift range of  $^{19}\text{F}$  signals (typically 100 kHz) compared with the relatively modest line width of most signals (<3 Hz) gives the potential to separate signals from more than 30,000 separate entities. Even greater selectivity can be conferred by recent developments that have successfully interfaced LC chromatographs with NMR instruments. LC-NMR technology is still under development and all the major NMR instrument manufacturers offer LC-NMR probes as standard accessories. First generation of LC-NMR probes were often re-tunable to  $^{19}\text{F}$  and, as we will see later, there are several examples where  $^{19}\text{F}$ -detected LC-NMR has been used to identify chromatography peaks of interest prior to  $^1\text{H}$  NMR analysis. Sadly, the drive to improve NMR sensitivity for  $^1\text{H}$  observation has resulted in a generation of probes that cannot observe  $^{19}\text{F}$  and will necessitate the special manufacture of  $^{19}\text{F}$  observe LC-NMR probes. NMR is a concentration detector; this infers that signals from small amounts of material will be obtained if the volume of the analyte solution is small enough. In the context of  $^{19}\text{F}$  analysis, using an LC-NMR probe with a detect volume of (say) 60  $\mu\text{l}$  it is possible to detect fluorinated substances, in real time, at levels of a few micrograms as the sample peaks pass from the LC through the NMR probe. Although presently limited to  $^1\text{H}$  NMR, NMR flow probes with ultra-small detection volumes (<2  $\mu\text{l}$ ) are at the point of production [61]; they are capable of generating good quality spectra of glucose at nanomolar concentrations (0.24  $\mu\text{g}$  in cell) within 10 min. This cell size is compatible with the

peak volumes in capillary LC and CE. The publication by Olson et al. [75] compares the efficiency of this microprobe with other NMR micro-detection devices.

Except when extreme detection limits are required, the combined use of MS and NMR is a viable and indeed an essential part of chemical structure determination. For the amounts of analyte typically available from organic synthesis, or following enrichment, MS and NMR can be used as a triply hyphenated technique along with LC (i.e. LC-MS-NMR) as described in the paper by Bailey [6].

## 2 Topical Applications of $^{19}\text{F}$ NMR Spectrometry

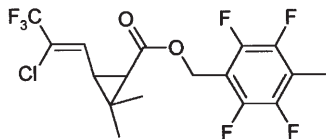
Many examples could be given, but this would involve a massive undertaking that is not the primary objective of this volume. Instead, the structural determination of a specific compound is discussed in detail as an illustration of the possibilities opened up by  $^{19}\text{F}$  NMR. It is appropriate to note that applications in microbiology, where no theoretical background is presented, are discussed elsewhere in this volume: likewise the many applications involving perfluorinated compounds are not considered, since they are discussed elsewhere in this volume.

### 2.1 Structure Elucidation – Tefluthrin, a Case Study

Tefluthrin (Table 5) is an insecticide used to control a wide range of soil insect pests, particularly those of the orders Coleoptera, Lepidoptera and Diptera, in maize, sugar beet, wheat and other crops. The analysis of residues is a central issue that determines the acceptability of agrochemicals, and for tefluthrin no residues (at a limit of detection 0.01 mg/kg) have been found in major crops treated at recommended rates.

The NMR spectra discussed below show how a range of experiments might be used in combination to successively refine the interpretation and assignment of the spectra of this commercially significant compound. These procedures may be regarded as hierarchical. All spectra were run on Varian Inova 400 MHz spectrometers. Figures 2–5 were acquired in our own laboratories (two-chan-

**Table 5.** Tefluthrin



2,3,5,6-Tetrafluoro-4-methylbenzyl (Z)-(1*RS*,3*RS*)-3-(2-chloro-3,3,3-trifluoroprop-1-en-yl)-2,2-dimethylcyclopropanecarboxylate

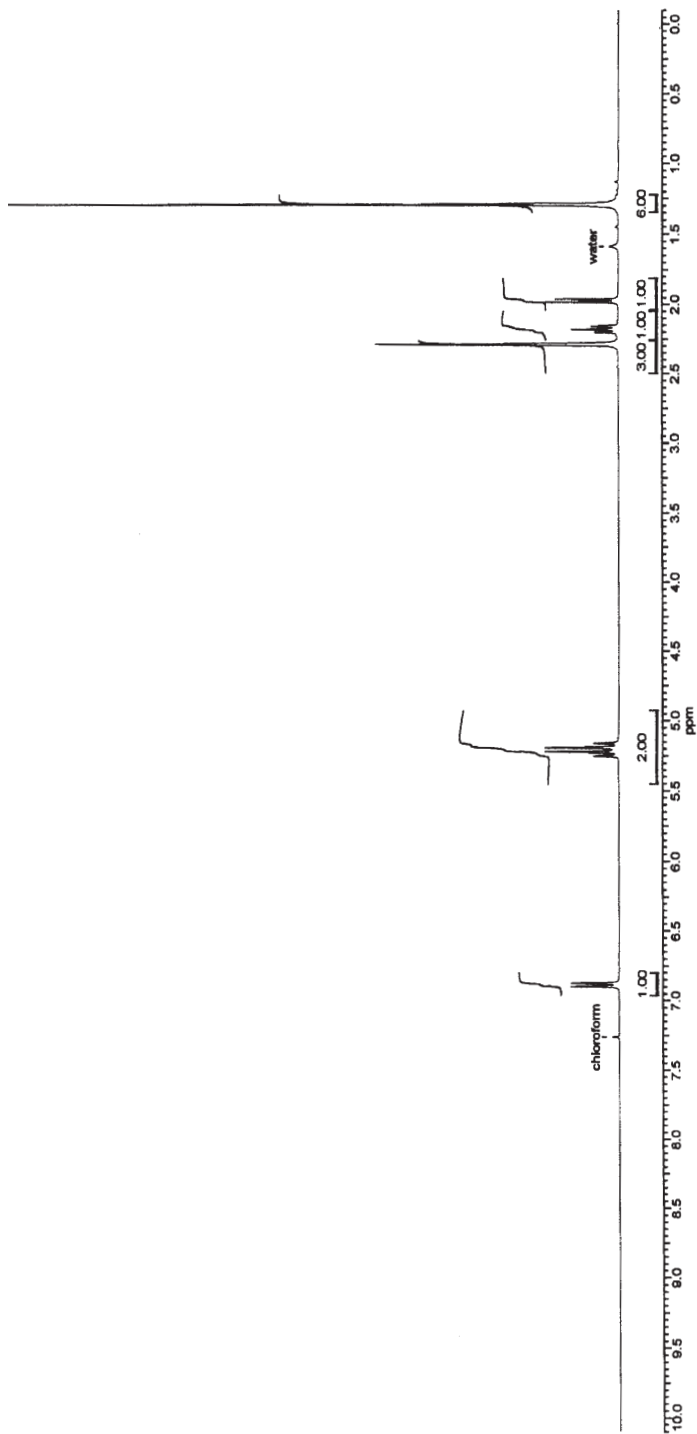


Fig. 2.  $^1\text{H}$  spectrum of tefluthrin

**Table 6.** Assignment of proton NMR spectrum of Tefluthrin

Chemical shift ( $\delta$ )	Integral (protons)	Description <sup>a</sup>	Coupling constant (Hz)	Assignment
6.89	1	bd	$^3J_{\text{HH}}$ 9.4	Propene 1- <i>H</i>
5.24	1	bd	$^2J_{\text{HH}}$ 12.1	Benzyl $\text{CH}_2$ (one)
5.18	1	bd	$^2J_{\text{HH}}$ 12.1	Benzyl $\text{CH}_2$ (one)
2.29	3	t	$^4J_{\text{FH}}$ 2.1	Benzyl 4- $\text{CH}_3$
2.18	1	bt	$^3J_{\text{HH}}$ 9.4	Cyclopropane 3- <i>H</i>
1.97	1	d	$^3J_{\text{HH}}$ 9.4	Cyclopropane 1- <i>H</i>
1.30	3	s		Cyclopropane 2- $\text{CH}_3$ (one)
1.29	3	s		Cyclopropane 2- $\text{CH}_3$ (one)

<sup>a</sup> b = broad, s = singlet, d = doublet, t = triplet.

nel instrument) under automation, the remainder by Dr Péter Sándor at the Varian application laboratory in Darmstadt (three-channel instrument). In both, a 5-mm AutoSwitchable probe was used (outer coil doubly tuned to  $^1\text{H}$  and  $^{19}\text{F}$ , inner coil doubly tuned to  $^{13}\text{C}$  and  $^{31}\text{P}$ ). No additional hardware, over and above the standard Inova configuration, was required, and the pulse sequences are from the standard Varian pulse library. The sample was prepared as a 20 mg/ml solution in chloroform-*d* to ensure reasonably fast acquisition times.

The proton NMR spectrum (Fig. 2) shows all the features expected from an NMR spectrum, i.e. chemical shifts indicating the presence of a range of chemical environments, integration traces showing the relative number of protons in each chemical environment and spin-spin coupling constants giving information on nearby  $^1\text{H}$  and  $^{19}\text{F}$  nuclei. Under normal circumstances, and only with the benefit of hindsight, this spectrum is sufficient to confirm that the sample is tefluthrin. The analysis of the proton spectrum is shown in (Table 6).

An important feature of this spectrum is that the  $^{19}\text{F}/^1\text{H}$  spin-spin couplings observed in this spectrum are all transmitted over four chemical bonds ( $^4J$ ) and, in the main, are observed only as a broadening of the relevant proton signals and are therefore not diagnostic. The stereochemistry of the *trans*-cyclopropane ring is "confirmed" by the magnitude of the  $^3J_{\text{HH}}$  coupling constant; in the case of *cis*-cyclopropanes in this class of substance,  $^3J_{\text{HH}}$  is typically 5–6 Hz. The (*Z*) stereochemistry of the propene substituent is substantiated by the chemical shift of the alkene proton; in the case of (*E*) propenes in this class of compounds, the alkene proton is shifted to higher field. Although this type of analysis is readily carried out for a known class of compound, this example serves to illustrate that *no real investigative analysis* has actually been performed.

The proton decoupled carbon spectrum and DEPT analysis (Figs. 3 and 4) add to the certainty of the structural assignments. The ACD spectrum prediction of the structure (Fig. 5) shows some small deviations from the observed spectra, attributable to the use of incomplete models in the prediction database.

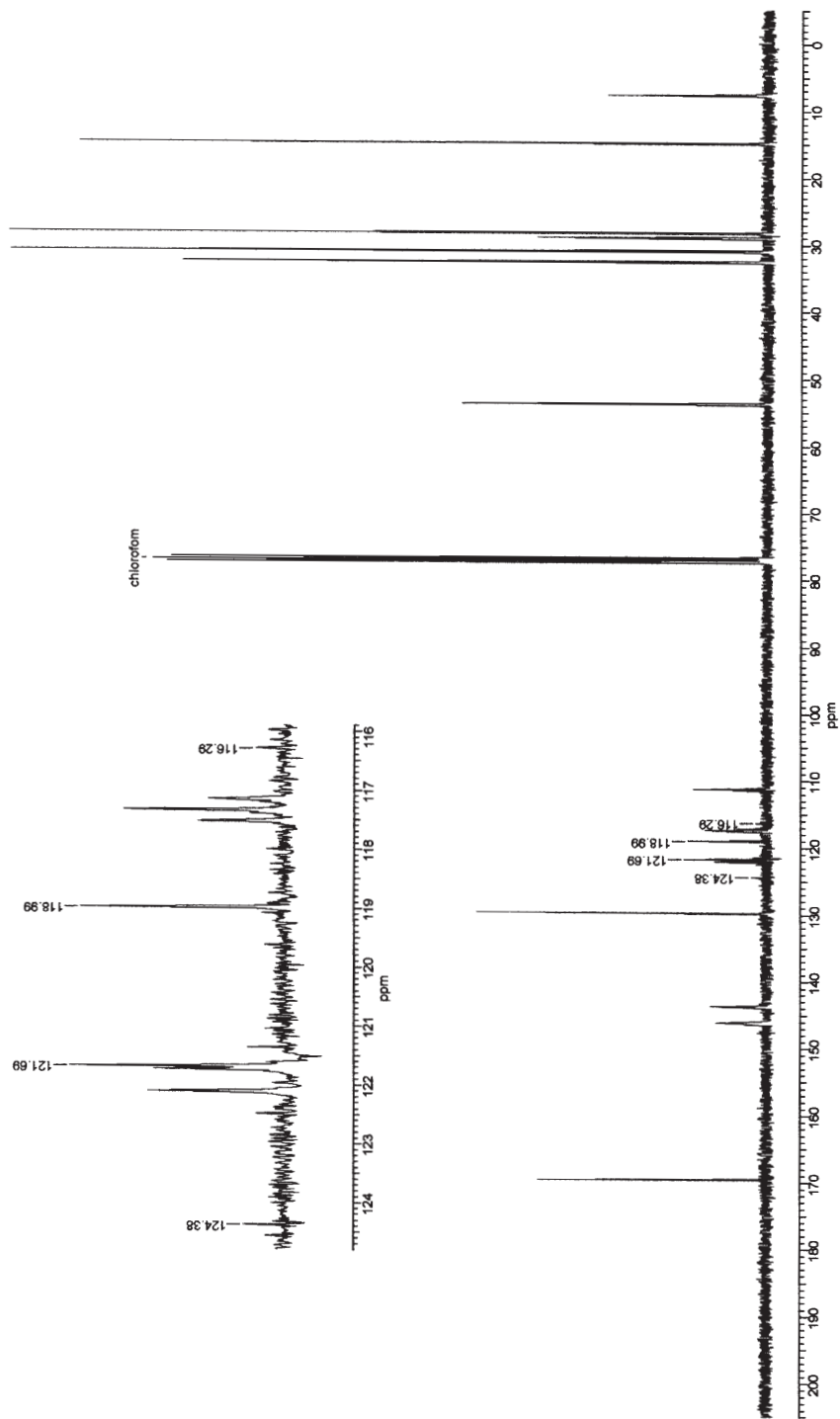


Fig. 3.  $^{13}\text{C}$  spectrum of tefluthrin; the inset shows an expansion of the aromatic region with the  $\text{CF}_3$  peak picked

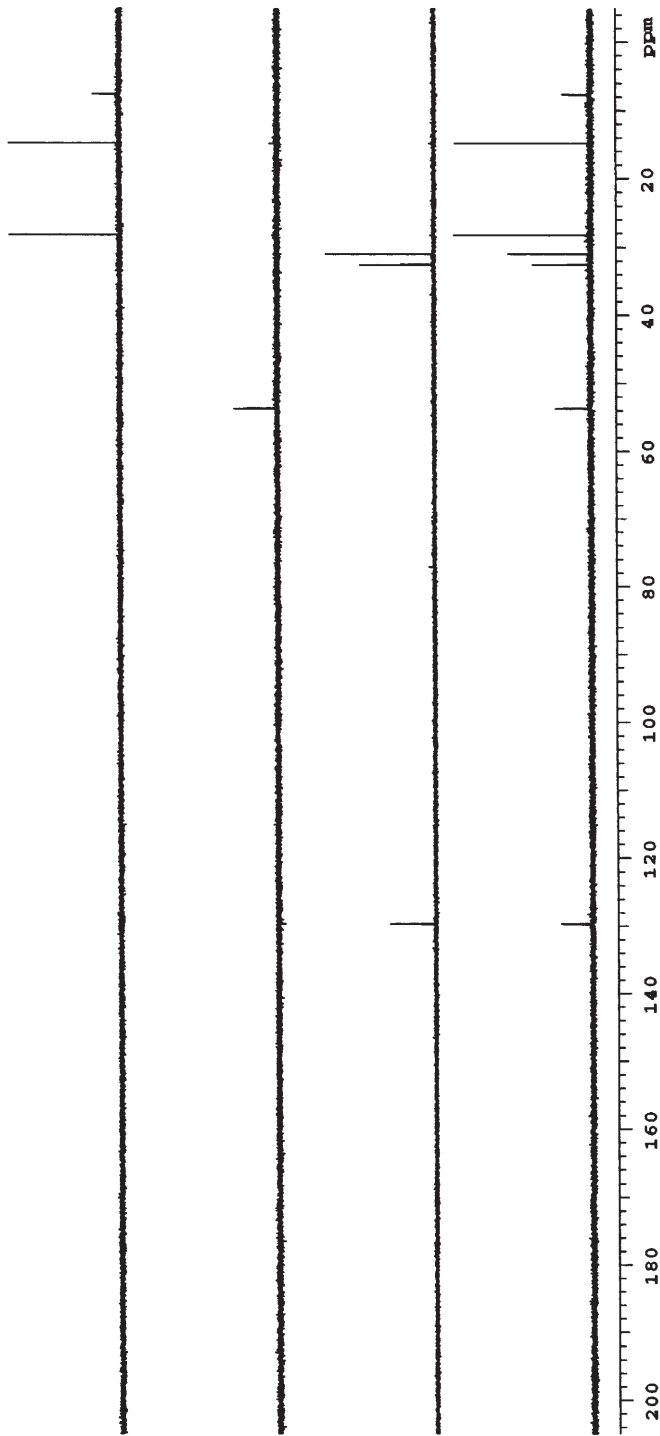
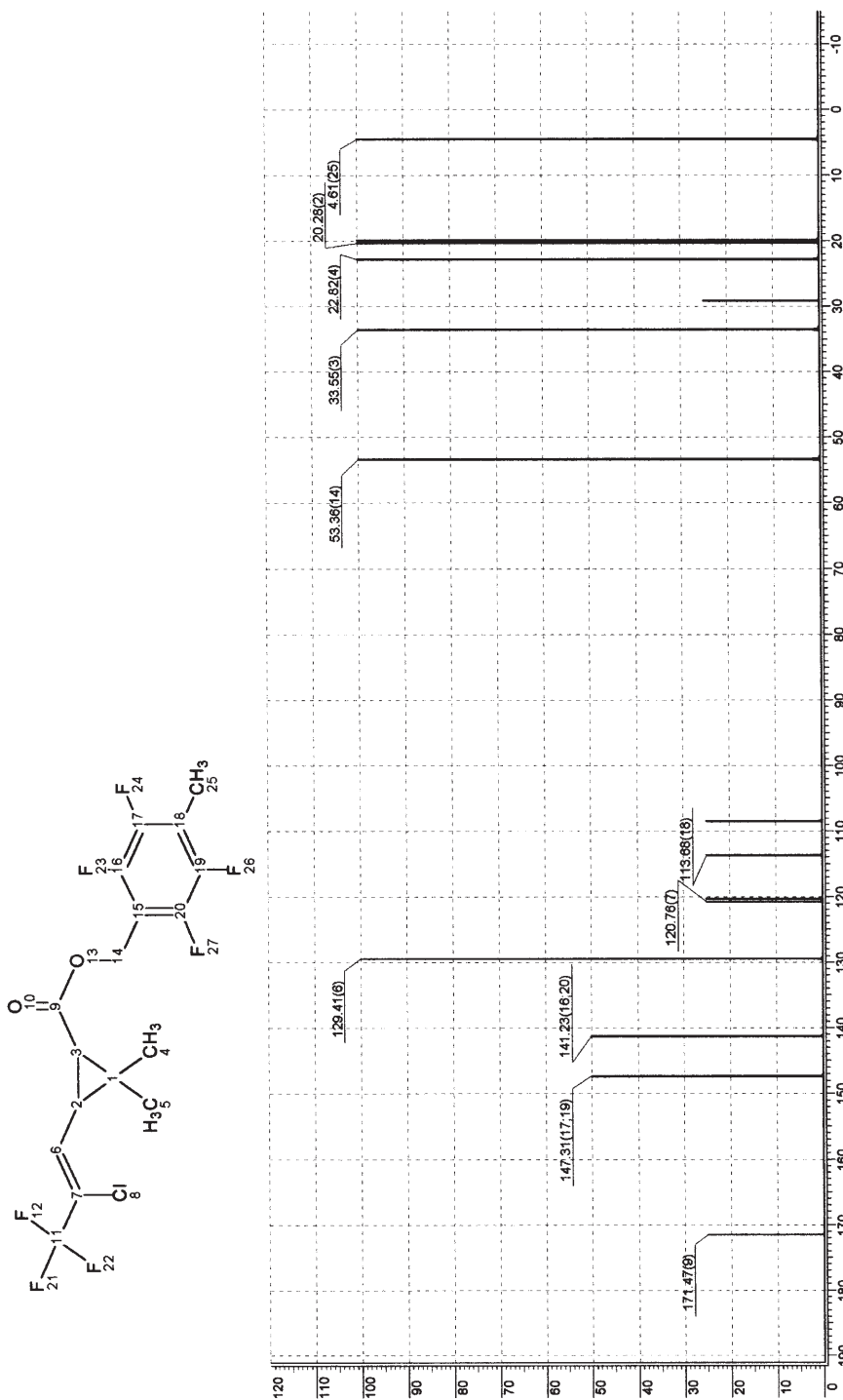


Fig. 4. DEPT edited  $^{13}\text{C}$  spectra of tefluthrin showing (*from bottom to top*): all protonated carbons, only CH carbons, only  $\text{CH}_2$  carbons and only  $\text{CH}_3$  carbons

Fig. 5. ACD prediction of  $^{13}\text{C}$  spectrum of tefluthrin

**Table 7.** Assignment of carbon NMR spectrum of Tefluthrin

Chemical shift ( $\delta$ )	DEPT <sup>a</sup>	Coupling constant $J_{FC}$ (Hz)	Assignment	ACD prediction ( $\delta$ )	$\Delta_{ACD-exp}$
169.7	S		COO	171.8	2.1
145.0	S	Complex	Benzyl 2,3,5&6-C	147.3	-0.1
129.7	D	$^3J_{CCCF_3}$ 4.5	Propene 1-C	129.4	-0.3
122.3	S	$^2J_{CCF_3}$ 37.6	Propene 2-C	120.8	-1.5
123.0	S	$^1J_{CCF_3}$ 271.0	CF <sub>3</sub>	120.3	-2.7
117.3	S	$^2J_{CCF}$ 18.4	Benzyl 4-C	113.7	-3.6
110.8	S	$^2J_{CCF}$ 17.7	Benzyl 1-C	108.5	-2.3
53.7	T		CH <sub>2</sub> COO	53.5	-0.2
32.5	D		Cyclopropane 1-C	33.5	1.0
31.0	D		Cyclopropane 3-C	20.3*	-10.7*
28.9	S		Cyclopropane 2-C	29.1	0.2
28.2	Q		Cyclopropane 2-CH <sub>3</sub>	22.8	-5.4
14.8	Q		Cyclopropane 2-CH <sub>3</sub>	19.9	5.1
7.7	Q		Benzyl 4-CH <sub>3</sub>	4.6	-3.1

<sup>a</sup> B=broad, S=singlet, D=doublet, T=triplet, Q=quartet denote the signal multiplicity reported by DEPT analysis (i.e. S is a quaternary carbon, D is a CH etc.). Coupling of the <sup>13</sup>C signals to <sup>19</sup>F is reported as text.

The large error in the prediction of the cyclopropane 3-C is an example of a program reporting error. The 32 models used to predict this chemical shift report an average value of 32.1 for this carbon atom, which represents an error of  $\Delta_{ACD-exp} - 1.1$  ppm. The vendors of this software are keen to improve the program code and therefore welcome these observations so that the program can be improved. In this case, spectrum prediction is a useful tool that will be used to design NMR experiments to clarify deficiencies in the incomplete models. The analysis of the carbon spectrum is shown in Table 7.

It is worth noting that the spin-spin couplings from the CF<sub>3</sub> and aromatic fluorine nuclei are visible in the proton decoupled carbon spectrum. The magnitudes of these spin-spin couplings are useful markers that aid the assignment of individual signals and, with careful study, can be used to give conformational information. The signals from the benzyl 2,3,5 and 6-C appear as a single complex multiplet that is not interpretable.

The <sup>19</sup>F spectrum of tefluthrin (Fig. 6) shows signals consistent with CF<sub>3</sub> (d-69) and aromatic fluorine nuclei (d-144 and d-145) that are shown expanded in the inset. Under the IUPAC conditions for <sup>19</sup>F NMR acquisition, integration of these signals is not meaningful.

In this case, the substance was available in relatively large quantities and the previous data can be acquired reasonably quickly; all these data sets were acquired and processed within 1 h under total automation. When only smaller amounts of a sample are available, the <sup>19</sup>F-<sup>13</sup>C couplings that we used to infer structural information are an inconvenience since the spin-spin coupling reduces the intensity of the signal (e.g. the intensity of a triplet is only 50% that

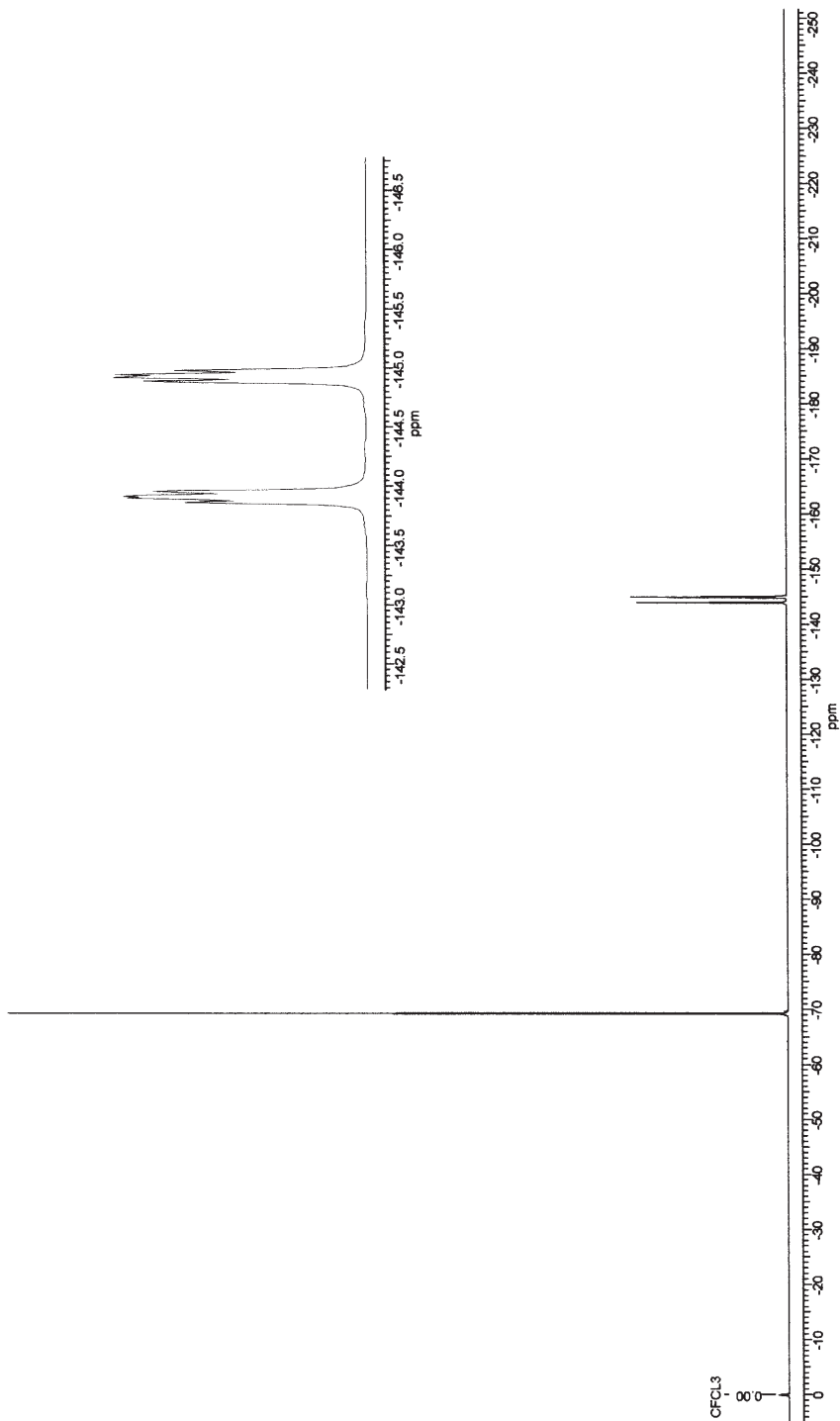


Fig. 6.  $^{19}\text{F}$  spectrum of tefluthrin; the *insert* shows expansion of aromatic fluorine signals

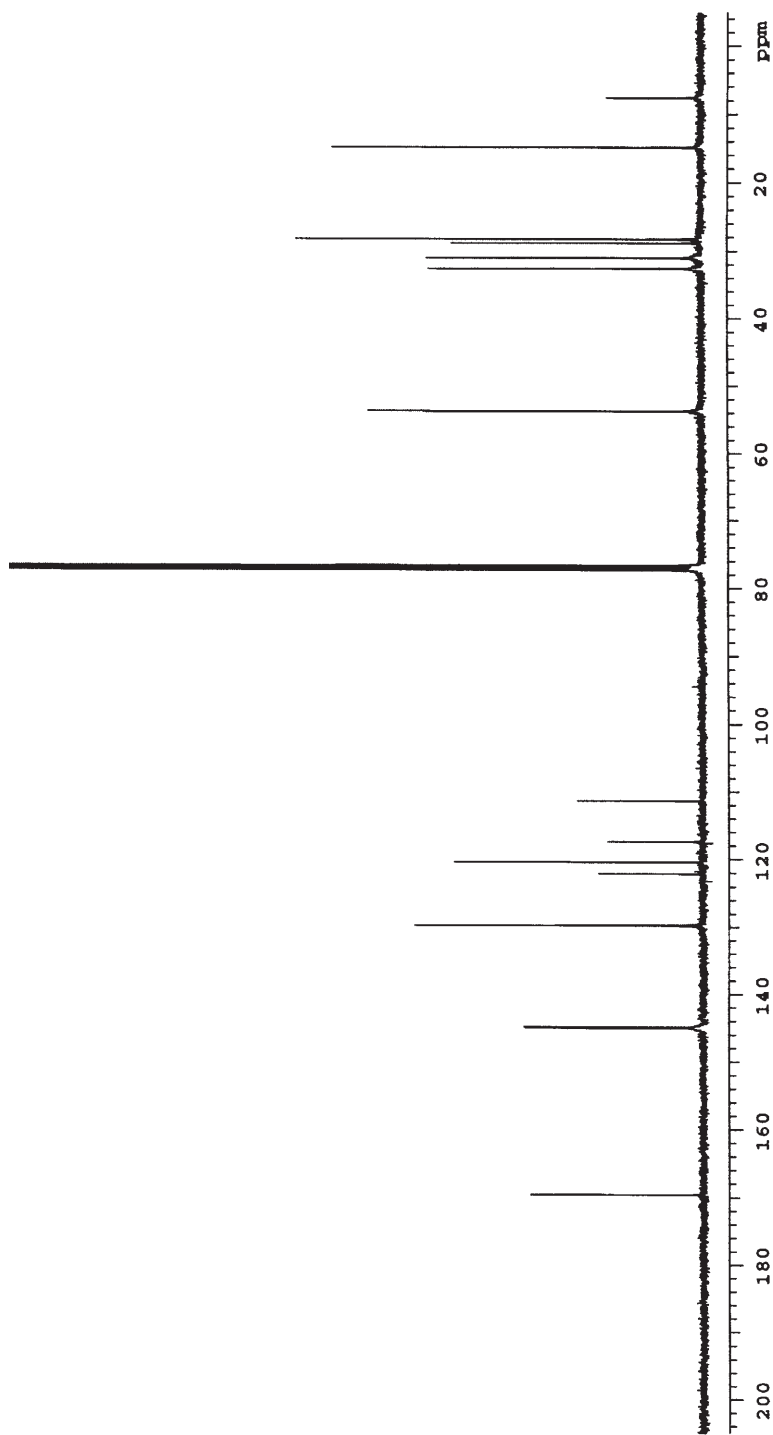
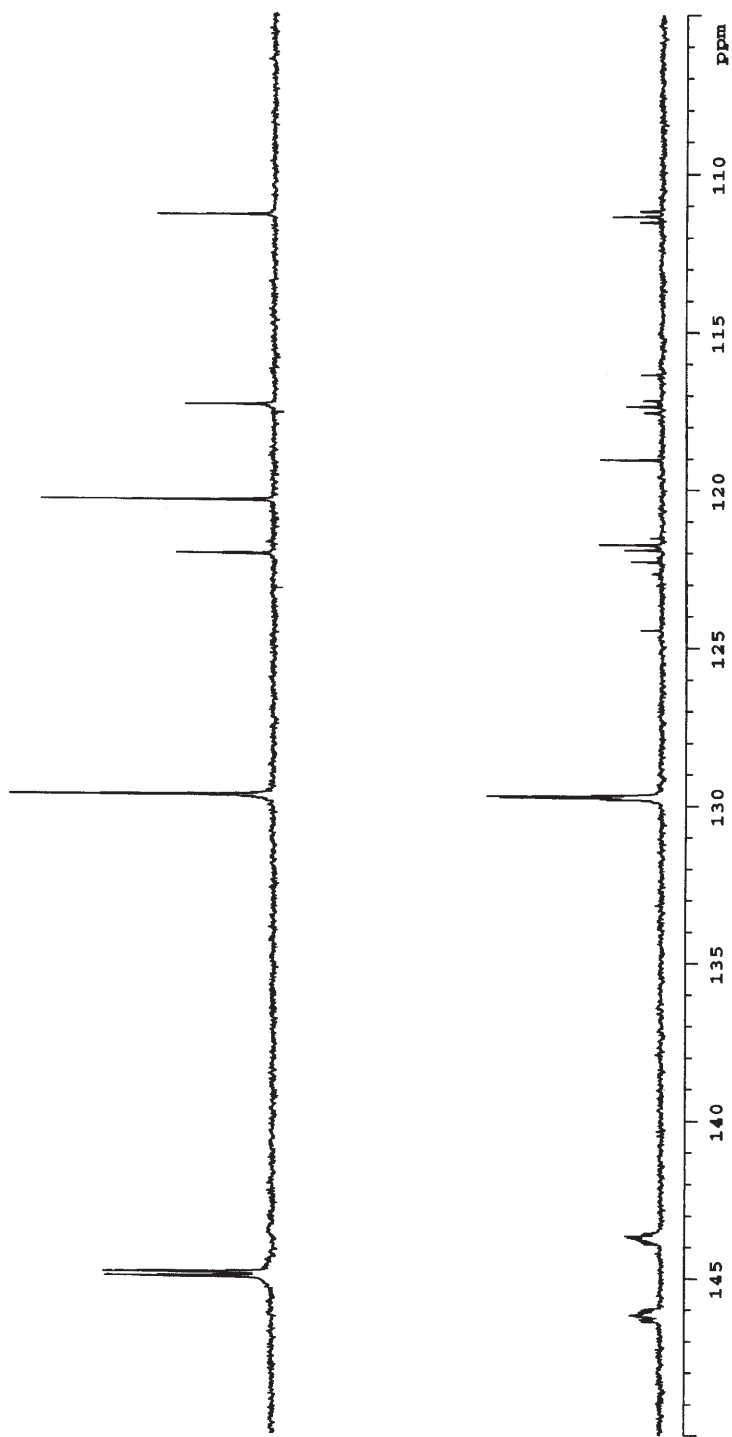
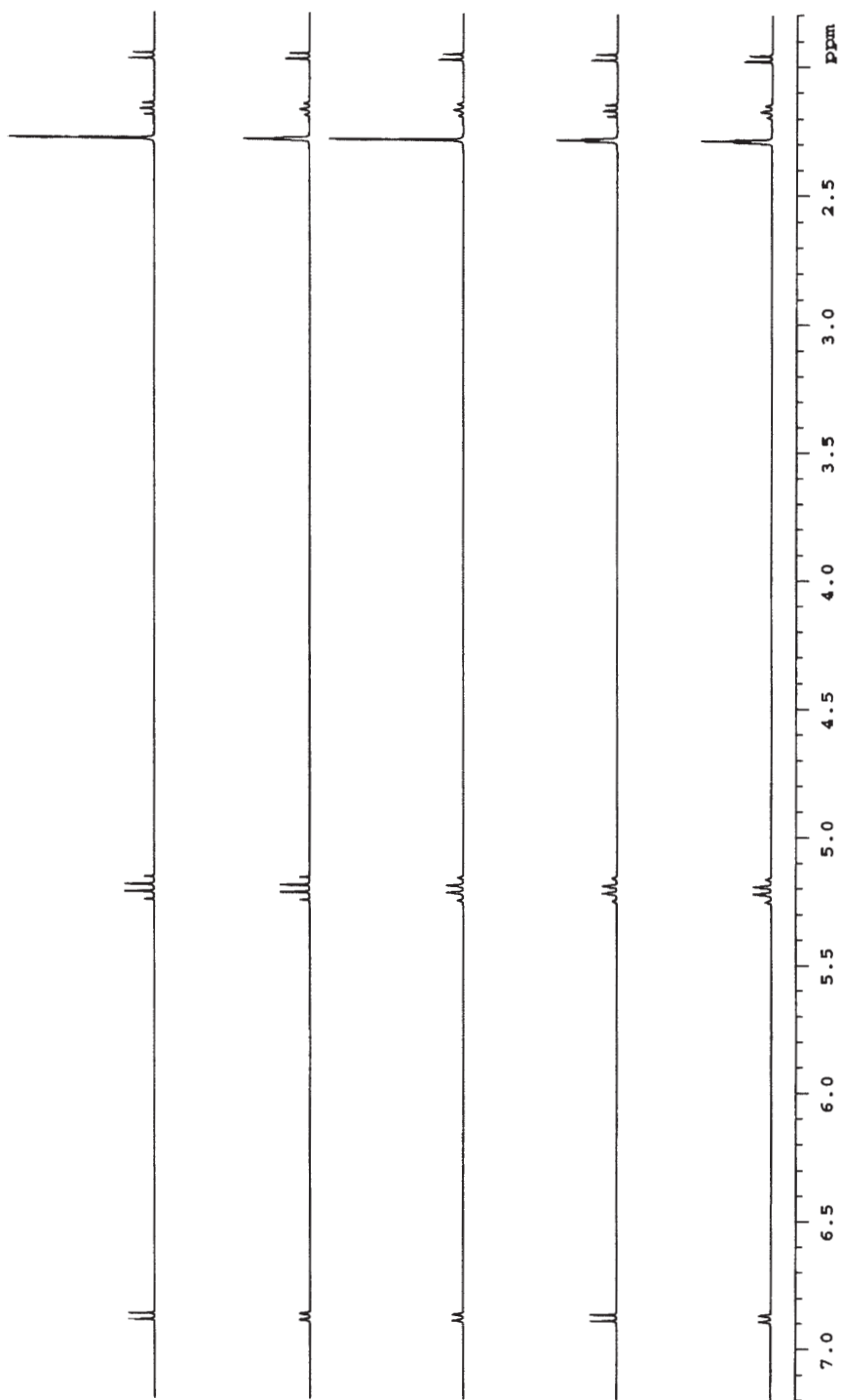


Fig. 7.  $\{^1\text{H}/^{19}\text{F}\}^{13}\text{C}$  spectrum of tefluthrin



**Fig. 8.** Expansion of aromatic regions of  $\{^1\text{H}\}^{13}\text{C}$  (*bottom*) and  $\{^1\text{H}/^{19}\text{F}\}^{13}\text{C}$  (*top*) spectra of tefluthrin showing simplification of fluorine coupled multiplets and resolution of signals at  $\delta$  145



**Fig. 9.**  $\{^{19}\text{F}\}^1\text{H}$  spectra of tefluthrin showing (from bottom to top): no irradiation, irradiation of  $\text{CF}_3$ , irradiation of aromatic 3 and 5-F, irradiation of aromatic 2 and 6-F and broadband decoupling

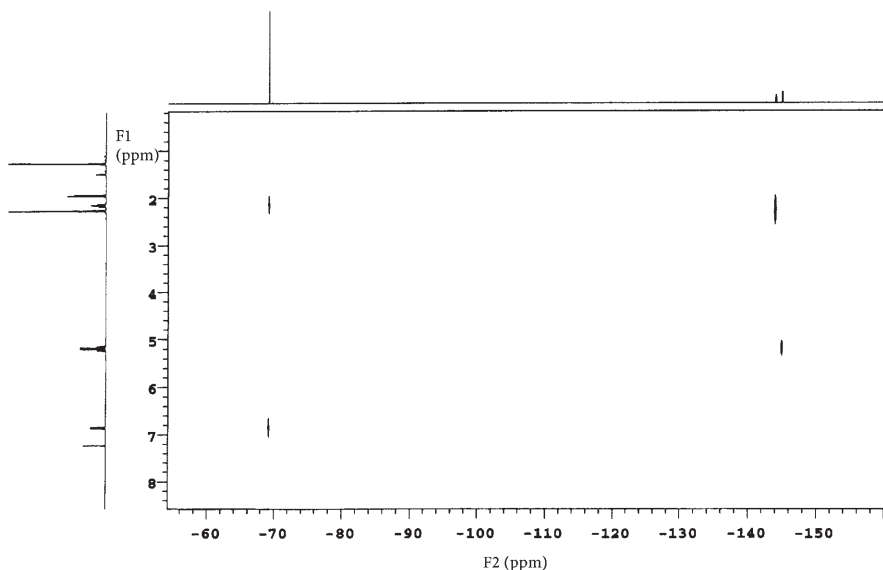


**Fig. 10.** Fluorine detected  $^{19}\text{F}$ - $^1\text{H}$  g-HMBC spectrum of tefluthrin

of the uncoupled signal). In such cases, where there is a suspicion that fluorine may be present, it is preferable to acquire preliminary data with both  $^{19}\text{F}$  and  $^1\text{H}$  decoupling as shown in Fig. 7.

Figure 8 is an expansion of the aromatic carbon region of the  $\{^1\text{H}\}^{13}\text{C}$  and  $\{^1\text{H}-^{19}\text{F}\}^{13}\text{C}$  spectra. In addition to an increase in the signal to noise ratio, the  $\{^1\text{H}/^{19}\text{F}\}^{13}\text{C}$  spectrum shows that the complex multiplet at d145 can be resolved into two separate signals representing the benzyl 2 and 6, and benzyl 3 and 5 carbons.

In the original proton spectrum we inferred the presence of the long-range  $^1\text{H}$ - $^{19}\text{F}$  spin-spin couplings that were expected in this substance through broadening of the coupled proton signals. When run under conditions of higher digital resolution these couplings are visible as shown in Fig. 9. This figure also illustrates a series of selective decoupling experiments that confirm the coupling pathways in the original assignment of the proton spectrum. This technique is selective enough to enable separate irradiation of the two signals from the aromatic fluorine nuclei, and confirms that the signal at  $\delta$ -144 in the fluorine spectrum represents the benzyl 3 and 5 fluorines.

The same information is conveyed more graphically in the gradient selected  $^1\text{H}$ - $^{19}\text{F}$  HMBC spectrum shown in Fig. 10.

In this spectrum, spin-spin couplings are displayed as correlation “islands” in the 2D spectrum. Thus the fluorine signal at  $\delta$ -144 (F2 dimension) shows a correlation with the proton signal at  $\delta$ 1.97 (F1 dimension) that represents the benzyl 4- $\text{CH}_3$ . The  $\text{CF}_3$  signal shows correlations with both the propene 1- $H$  and the cyclopropane 3- $H$  that represents spin-spin coupling through both three and four chemical bonds.

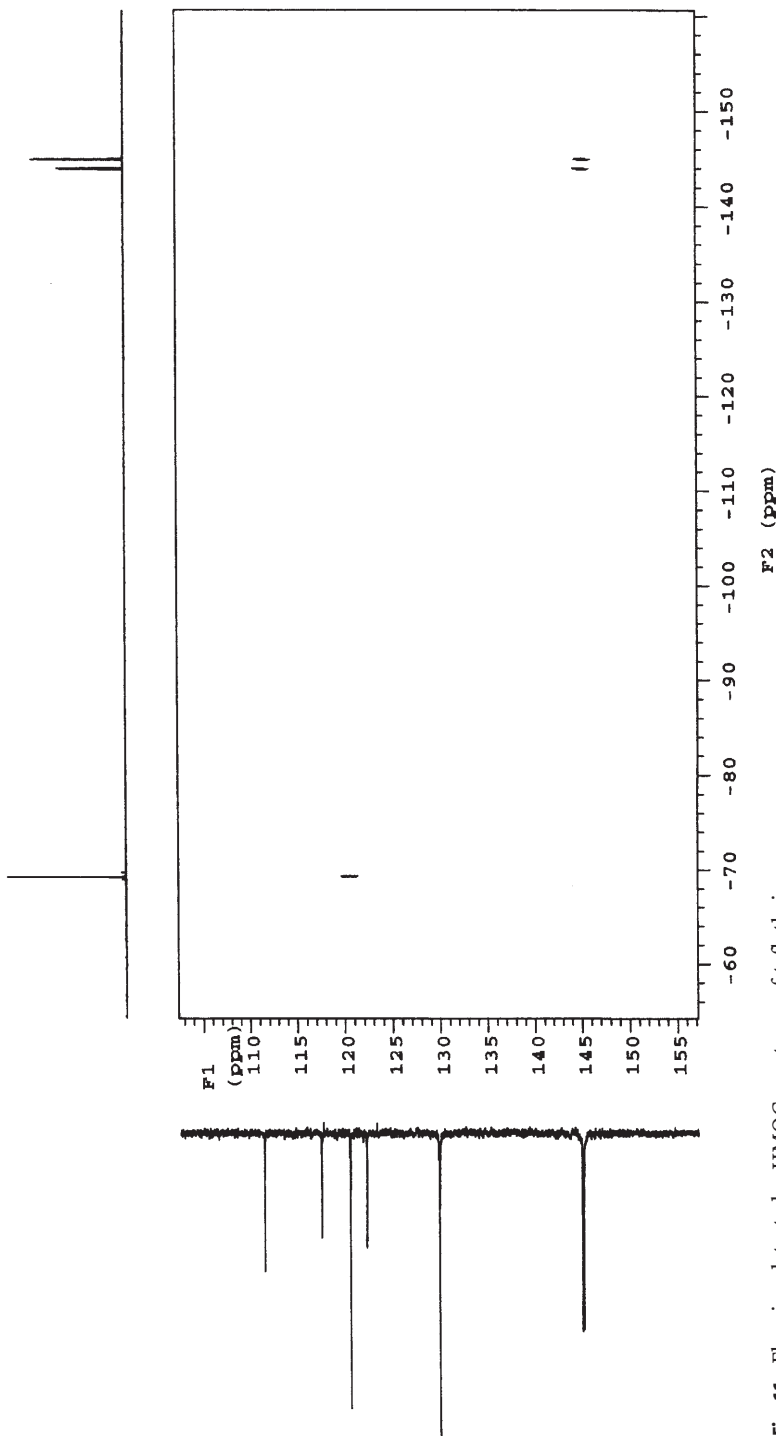


Fig. 11. Fluorine detected g-HMQC spectrum of tefluthrin

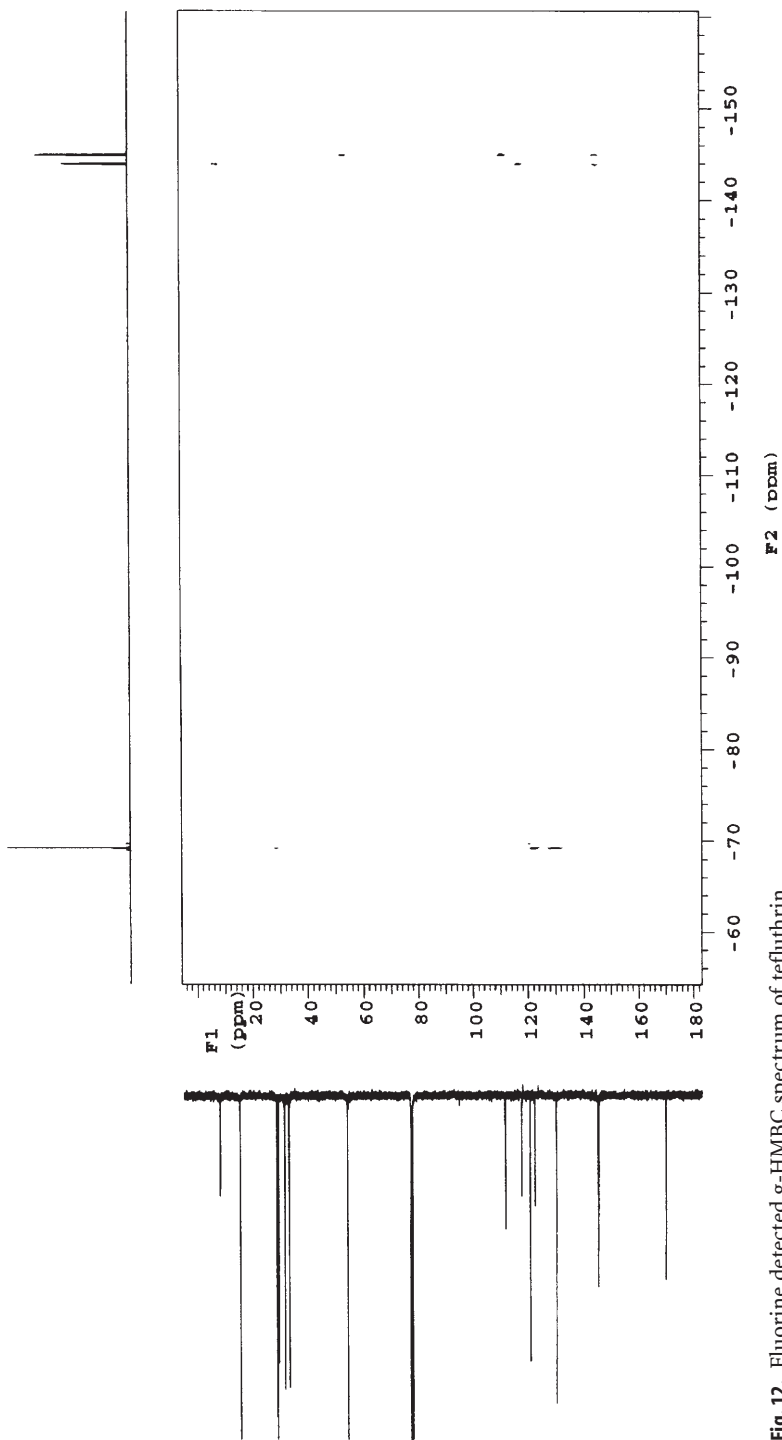


Fig. 12. Fluorine detected g-HMBC spectrum of tefluthrin

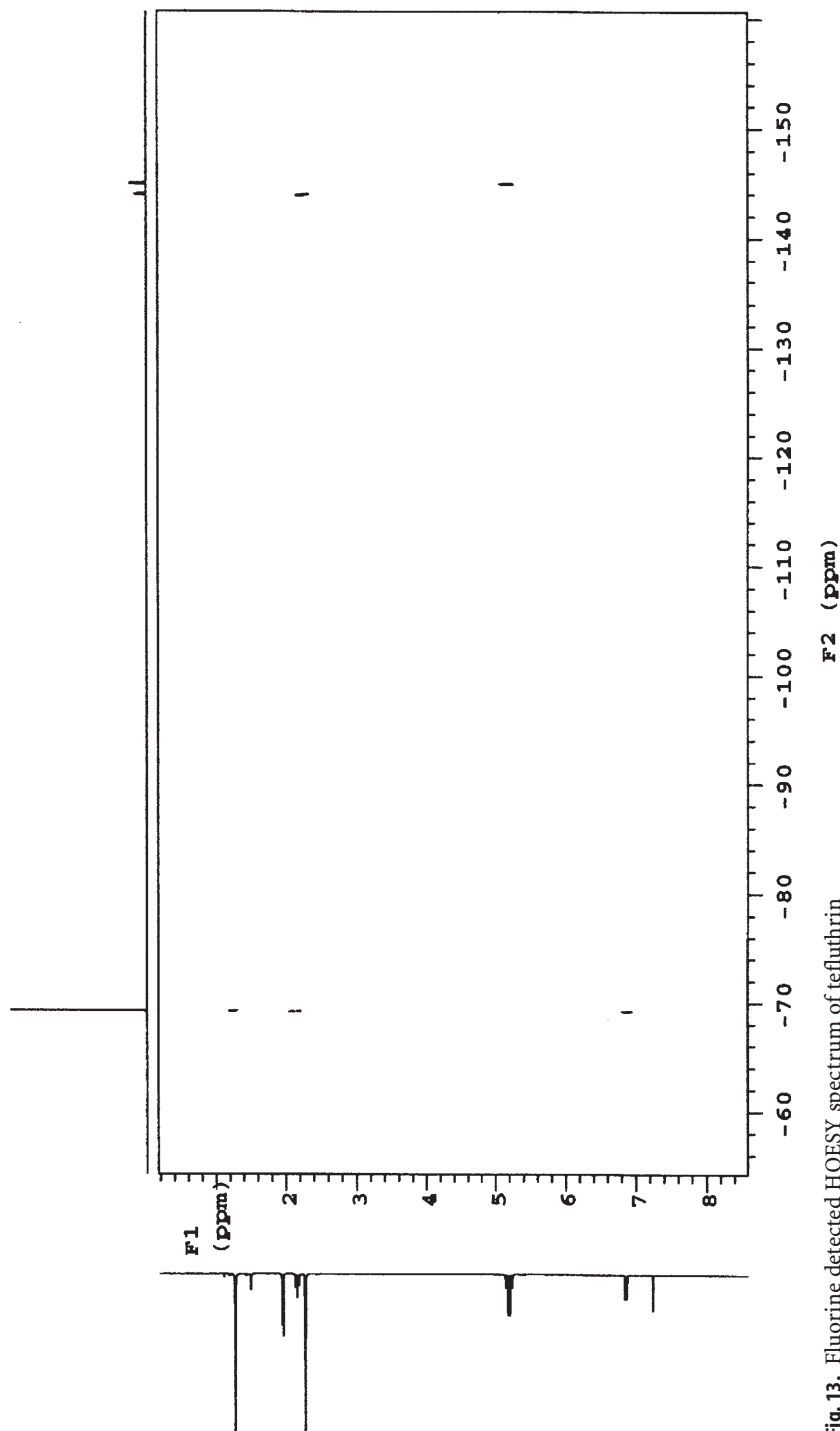


Fig. 13. Fluorine detected HOESY spectrum of tefluthrin

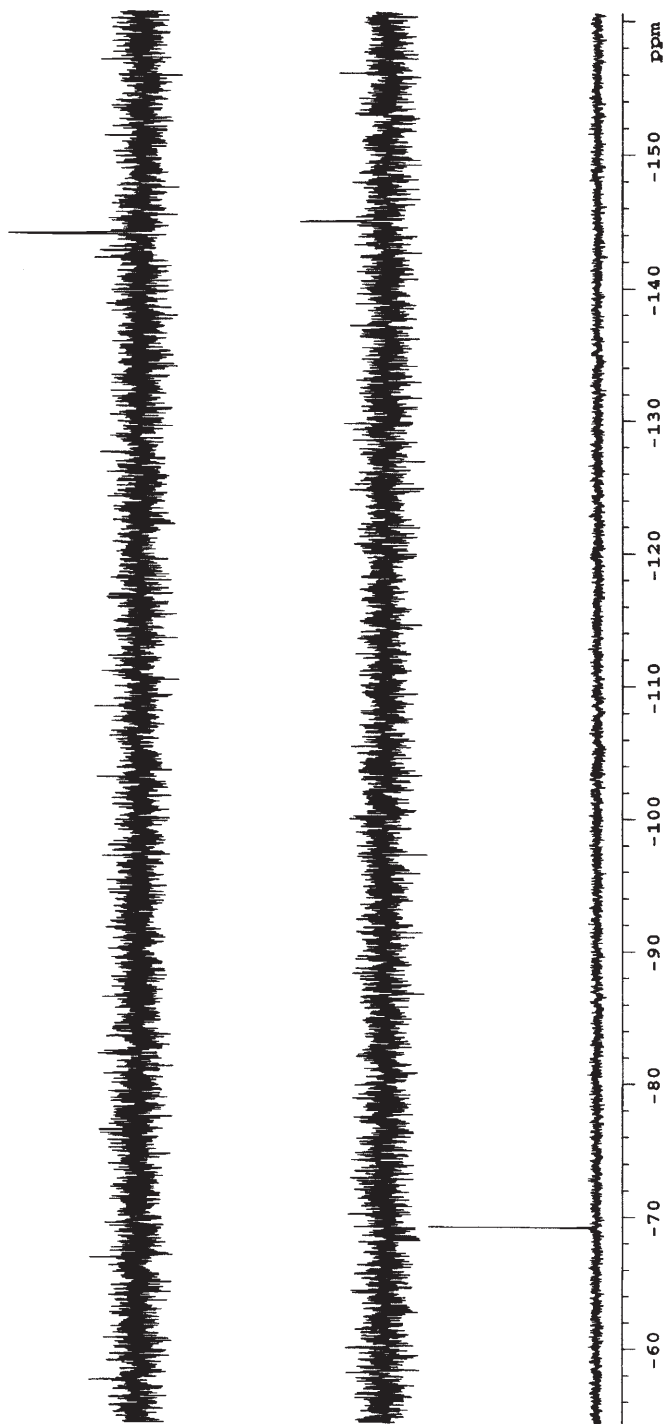


Fig. 14. Fluorine detected HETGOESY spectrum of tefluthrin, with selection (*from bottom to top*) of propene 1-*H*, benzyl C-4  $\text{CH}_3$  and benzyl C-1  $\text{CH}_2$

Figure 11 shows a gradient selected HMQC experiment optimised to determine one bond  $^{19}\text{F}$ - $^{13}\text{C}$  couplings (270 Hz) and confirms the assignment of the  $\text{CF}_3$  carbon. Interestingly, this experiment has sufficient resolution to discriminate between the two very close signals representing the fluorinated carbons in the benzyl group. Since they are so close, the result may seem academic but this is an interesting illustration of the capability of the technique.

The longer-range spin-spin couplings between  $^{19}\text{F}$ - $^{13}\text{C}$  are probed using the gradient selected HMBC spectrum shown in Fig. 12. For example, correlations representing couplings from the fluorine signal at  $\delta$ -144 can be seen to the carbon signals representing the benzyl 4-C, benzyl 2 and 6-C and the benzyl 4-C  $\text{CH}_3$ .

HOESY [85] is a 2D NMR experiment similar to NOESY that yields information on the spatial relationships between spins in the heteronuclear case. The primary use of this experiment is to determine distances between quaternary carbon atoms and protons where spin-spin coupling information is unhelpful. In this case, Fig. 13 shows the  $^1\text{H}$ - $^{19}\text{F}$  HOESY spectrum of tefluthrin, and proximity information between the fluorine signal at  $\delta$ -144 and the proton signal from the benzyl methyl group can be clearly seen.

Often 1D NOE methods are to be preferred, and the HETGOESY experiment [102] originally developed to detect  $^{13}\text{C}$ - $^1\text{H}$  NOE enhancements, detected directly on the  $^1\text{H}$  channel, can be adapted to  $^{19}\text{F}$  measurements. This experiment uses pulsed field gradients for coherence selection, thereby completely avoiding the problems associated with difference spectroscopy. In this adaptation, selective excitation is used in the better-resolved decoupled  $^{19}\text{F}$  spectrum rather than in the  $^1\text{H}$  spectrum (Fig. 14).

Although the information content of these spectra can be inferred from previous experiments, the sensitivity of this experiment is higher than with normal NOE methods, and the relatively small enhancements observed illustrate the problems associated with NOE measurements of small molecules. Using  $^{19}\text{F}$  detection minimises the number of artefacts in the spectra, allowing the easier identification of true correlations.

## 2.2

### LC/NMR and Metabolite Identification

The analysis of complex mixtures (e.g. biological fluids) using high resolution NMR spectroscopy has been successfully applied to the study of altered levels of endogenous substances in pathological conditions [74] and to the identification of xenobiotics and their metabolites [43].

Naturally, complex mixtures generate complex NMR spectra that require spectral editing techniques and 2D NMR methods to assign resonances [41, 103]. If the mixtures can be separated, or simplified, the task of structure elucidation becomes easier. When metabolites with a range of polarities are present, the partial separation of the components using solid phase extraction prior to NMR analysis has been applied successfully [110].

Ideally each component of the mixture should be separated, for example by chromatography, prior to NMR analysis. Attempts to develop coupled LC-NMR

started in the 1980s [8, 32] but were not widely adopted due the lack of sensitivity of the NMR detector and the expense incurred by the necessity of using deuterated LC solvents. Recent advances such as higher magnetic field strength, developments in NMR probe design, and solvent suppression techniques have resulted in major improvements in LC-NMR technology. As a result, it has become a viable tool for obtaining NMR spectra directly from the small (microgram) amounts of separated compounds delivered from an on-line chromatography system. With this amount of material, however, only proton, fluorine and proton detected heteronuclear correlation experiments (e.g. HMQC etc.) are possible. The world's major pharmaceutical businesses have been stimulated by these developments to undertake a major re-examination of the technique as a tool to solve a range of problems in biochemistry and drug metabolism. Despite aggressive investment in this area by industry, the major technical innovations in the area come from academia, for example, Nicholson's group at Imperial College (University of London).

Before we consider applications, it is important to recognize the operational choices and limitations of the LC-NMR technique. In its simplest form, the LC-NMR experiment involves the acquisition of NMR data from the effluent from the LC chromatograph that is used for separation of the components of the sample. The LC-NMR probe is designed to have a small volume (typically 60–100  $\mu\text{l}$ ) that is slightly smaller than the actual volume of solvent associated with a typical chromatography peak. This ensures that there are no concentration gradients across the NMR detection region in the probe leading to poor NMR line shape. With careful calibration of the instrument, NMR data from both isocratic and gradient elution regimes can be acquired successfully. LC-NMR experiments are almost exclusively limited to chromatography systems containing either water/acetonitrile or water/methanol mobile phases. The common practice is to use deuterated water ( $\text{D}_2\text{O}$ ) and protonated acetonitrile or methanol since  $\text{D}_2\text{O}$  is relatively cheap. The chromatography conditions required for successful LC-NMR are, however, often unlike those developed by a specialist chromatographer for purely analytical purposes. It is essential that the chromatography conditions are adjusted so that the peak of interest is well separated from closely eluting components. In addition, the chromatographic system should be tolerant of overloading since this condition is almost always required to ensure that sufficient material is present in the peak being measured by the NMR spectrometer. The major consideration in limiting the solvent system to a simple binary mixture is that the signals from the solvent, that appear as major peaks in the proton NMR spectrum, must be suppressed using a NMR pulse sequence. The resulting spectrum has areas that have been "burnt" out by the suppression process; more than two of these degrade the information content of the NMR spectrum to such an extent that the spectrum is useless. A recent review [98] describes recent developments in solvent suppression techniques and their application to LC-NMR.

The possible modes of NMR operation are on-flow analysis, stopped flow analysis, and the retrospective analysis of components recovered from sample storage loops. When small amounts of the analyte are involved, the acquisition of useful proton NMR data "on-flow" is not viable due to the low sensitivity of

even the highest field NMR spectrometer. “Stopped flow” analysis, where the chromatographic separation is paused during acquisition of the NMR spectrum (often for several hours), is far more widely used. To avoid possible degradation and diffusion of materials held on the chromatography column during these long periods of NMR spectrum acquisition, the chromatography is often carried out as normal except that the peaks of interest are transferred into sample storage loops. The contents of these loops can then be transferred sequentially to the NMR instrument for measurement. This method enables the NMR instrument to be used for other purposes whilst the chromatography is being completed.

Sensitivity is the keyword for LC-NMR experiments. LC-NMR probes are optimised for sensitivity by designing detection cells with good filling factors and good NMR line shape. Based on detection of mass, these probes are the most sensitive conventional probes available. The other factor in the equation is, of course, the NMR magnet field strength. The higher the magnetic field, the more sensitive the instrument. It is unlikely that successful LC-NMR experiments on low abundance substances will be carried out effectively with magnetic fields of less than 500 MHz, with 600 MHz being the industry standard. Fields in excess of this are desirable, but in the main often unaffordable.

Nicholson’s paper [100] was the first to report the use of  $^{19}\text{F}$  NMR in conjunction with LC. Whilst  $^{19}\text{F}$  NMR spectra contain little structural information, due to the absence of background signals, they are an ideal indicator of which peaks in a complex chromatogram represent fluorinated materials. This paper demonstrates the identification of the two major urinary metabolites of the anti-inflammatory drug Flurbiprofen: the glucuronide and 4’-hydroxyflurbiprofen, by a combination of on-flow  $^{19}\text{F}$  detected LC-NMR to identify the fluorine-containing chromatography peaks, followed by the acquisition of stopped flow  $^1\text{H}$  detected LC-NMR to enable structural characterization of the metabolites.

This principle may be illustrated with reference to plant metabolites [6]. 5-Trifluoromethyl-pyridone (5TFMP) serves as a simple substrate to examine the possible occurrence of *N*- vs *O*-glycosylation in plants. Following spiking with 5TFMP, the 500-MHz  $^1\text{H}$  NMR spectrum (Varian Inova 500) of a typical aqueous extract of maize (*Zea mays* L.) shoot material is shown in (Fig. 15). Apart from signals due to carbohydrates (d 5.45–3.20) the spectrum contains few interpretable peaks. The corresponding  $^{19}\text{F}$  NMR spectrum (JEOL GSX270) is shown in (Fig. 16). In this spectrum, the chemical shift scale was referenced using 3-trifluoromethyl-pyridone (3TMFP), and clearly shows the presence of four other fluorinated materials, identified as 5TFMP together with three putative metabolites.

The on-flow  $^{19}\text{F}$  NMR detected HPLC (Brüker DRX 500) chromatogram is shown in (Fig. 17), where the data are shown in “pseudo 2D” format representing several 1D  $^{19}\text{F}$  NMR spectra viewed from above, and acquired separately during a period of approximately 30–45 min during the elution of the chromatogram. It should be noted that the sensitivity of the experiment precludes the detection of a signal for the substance labelled “Metabolite III” in Fig. 16. From this data we conclude that the  $^{19}\text{F}$  NMR signal for “Metabolite I” is con-

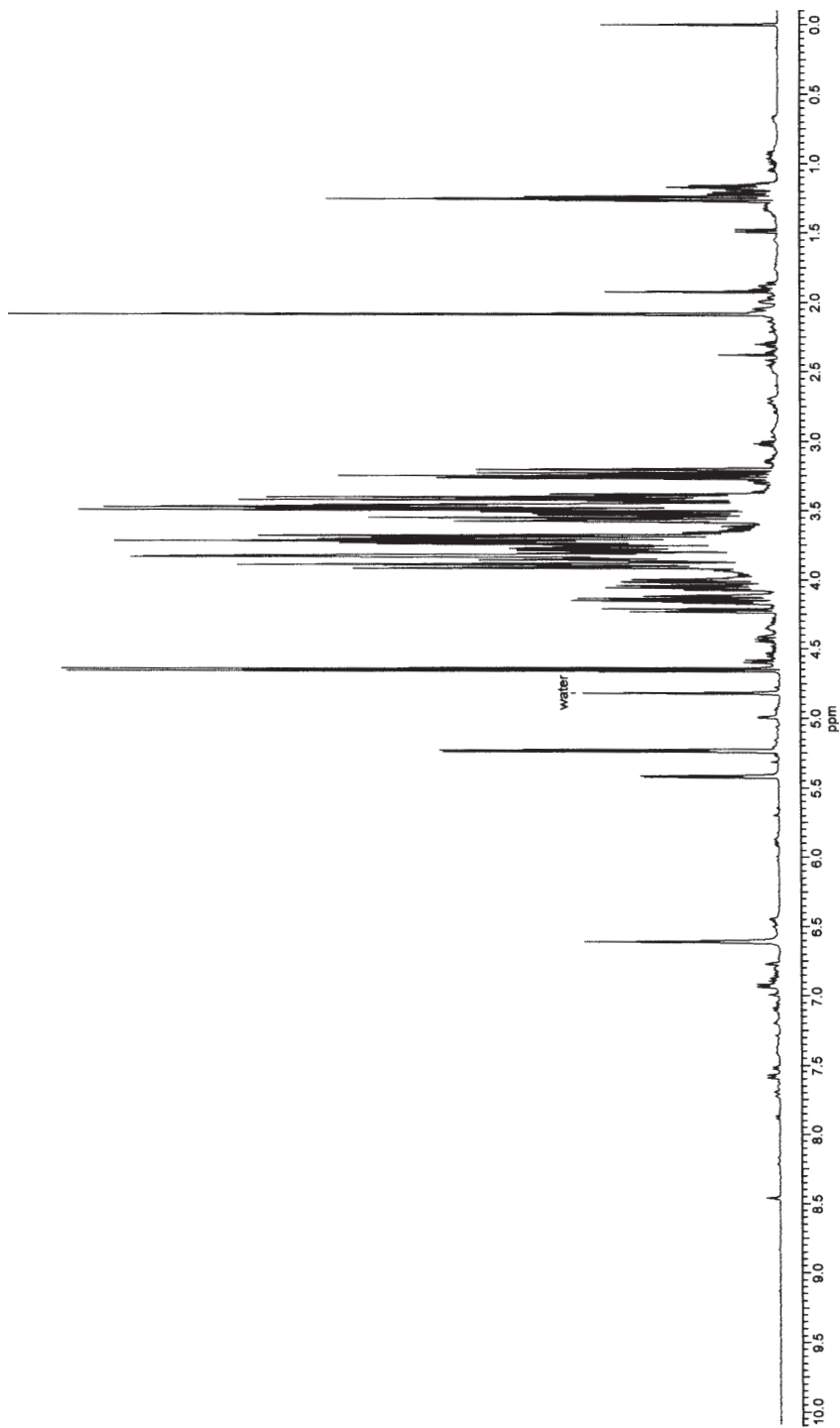


**Fig. 15.** 500 MHz Proton NMR spectrum of maize extract; residual peak from water signal suppression indicated at  $\delta$  4.8

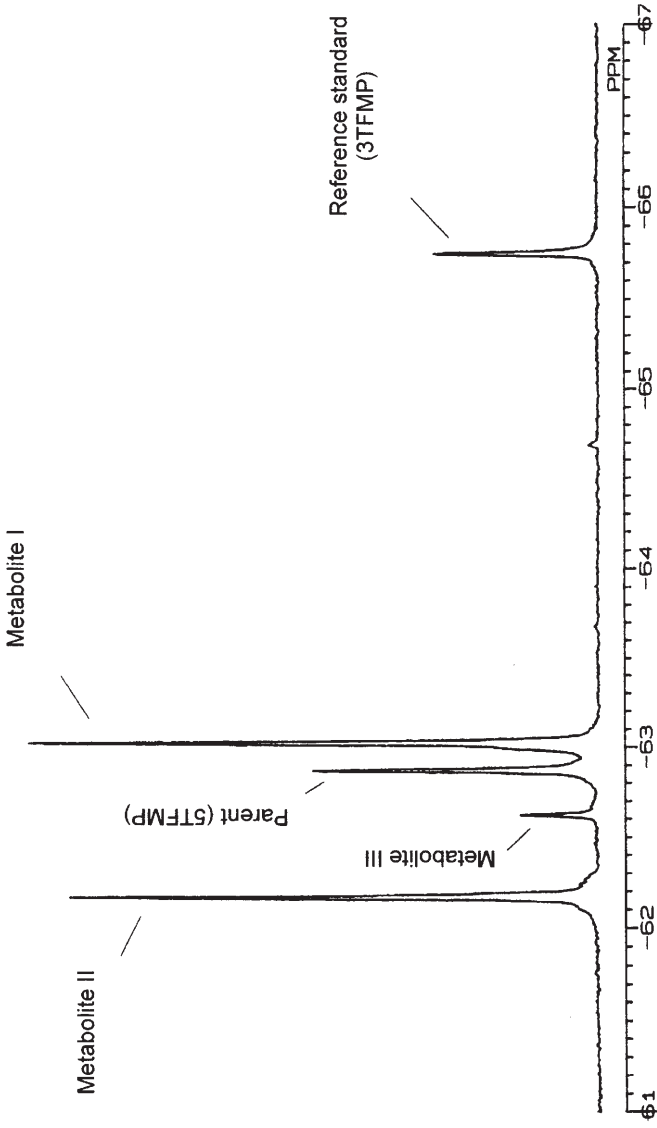
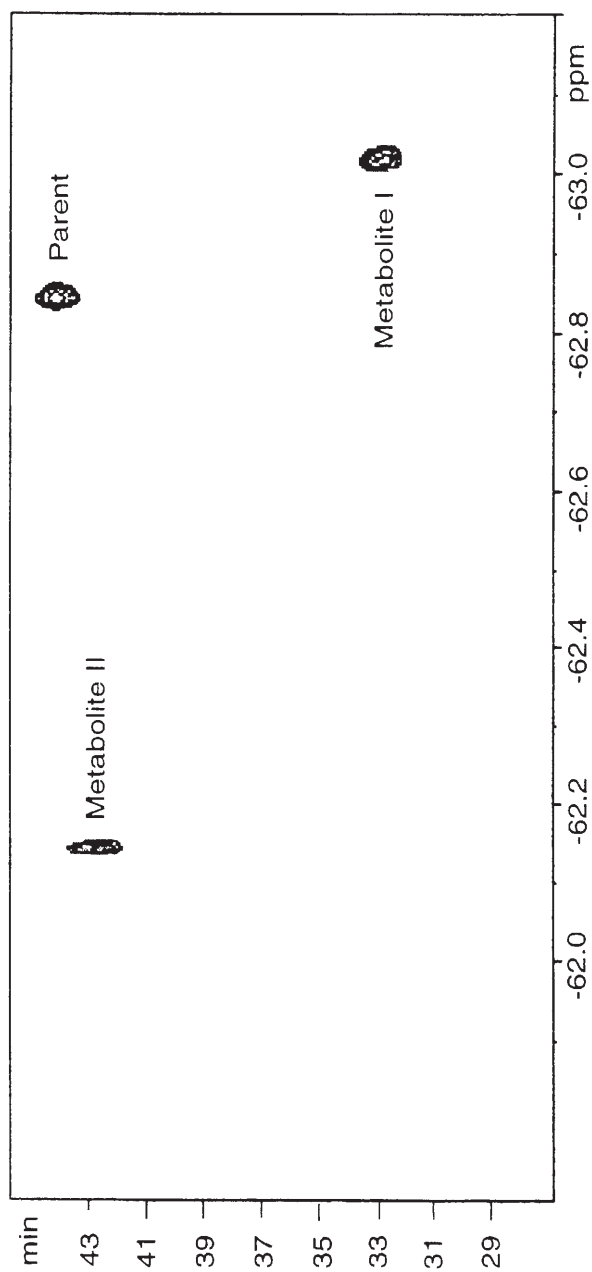


Fig. 16. 254.05 MHz <sup>19</sup>F NMR spectrum of maize extract 14 days after dosing with 5-trifluoromethyl-2-pyridone (5TFMP). Chemical shift referencing is to 3-trifluoromethyl-2-pyridone (3TFMP)



**Fig. 17.** On-flow 470.5 MHz  $^{19}\text{F}$  NMR detected HPLC chromatogram of maize extract after dosing with 5TMFP. Reproduced with permission from *J Agric Food Chem* (2000) 48(1):42–46, Copyright (2000) American Chemical Society

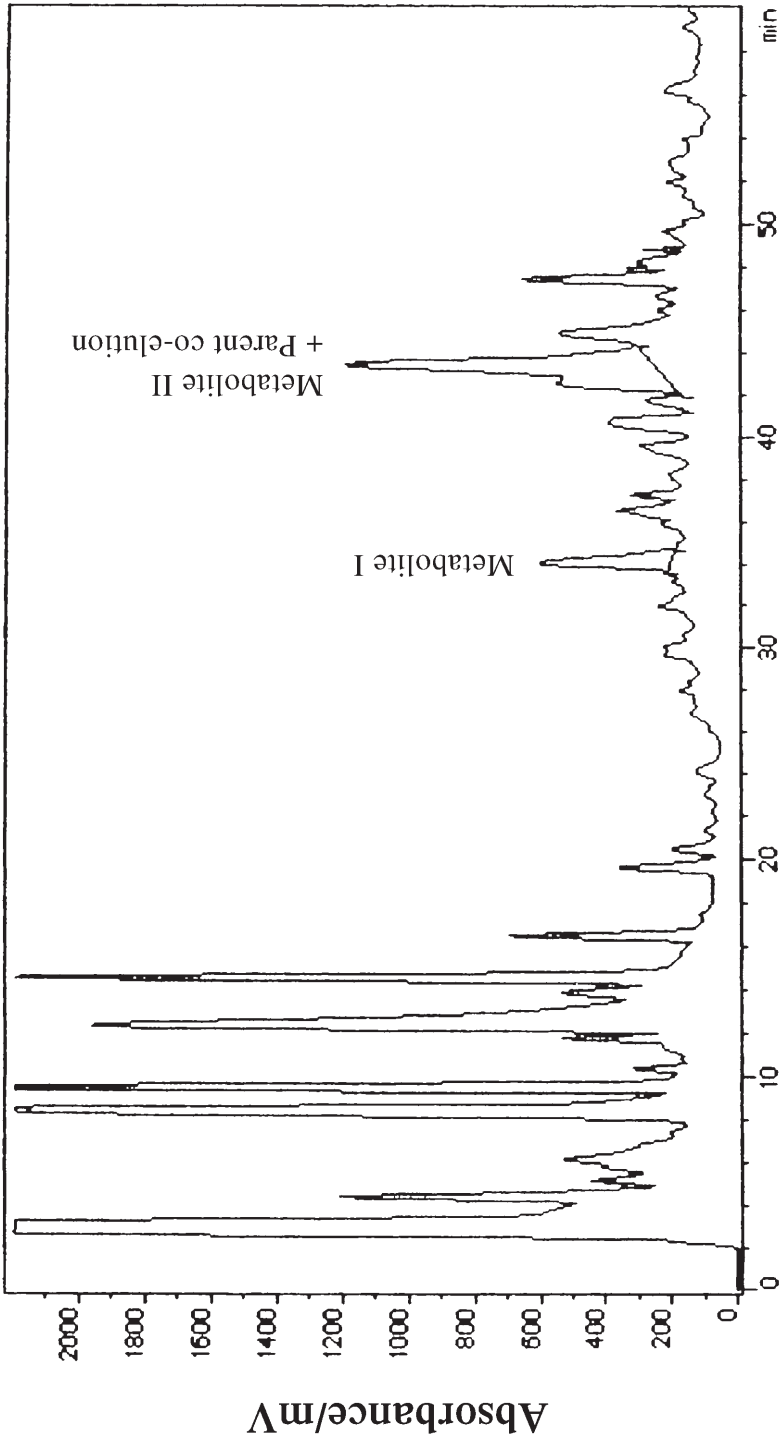
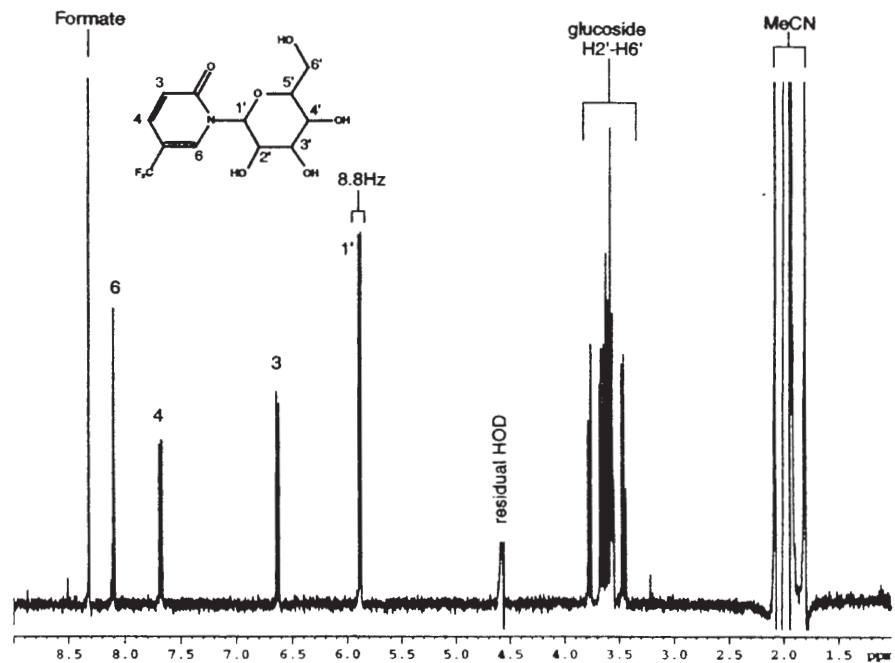
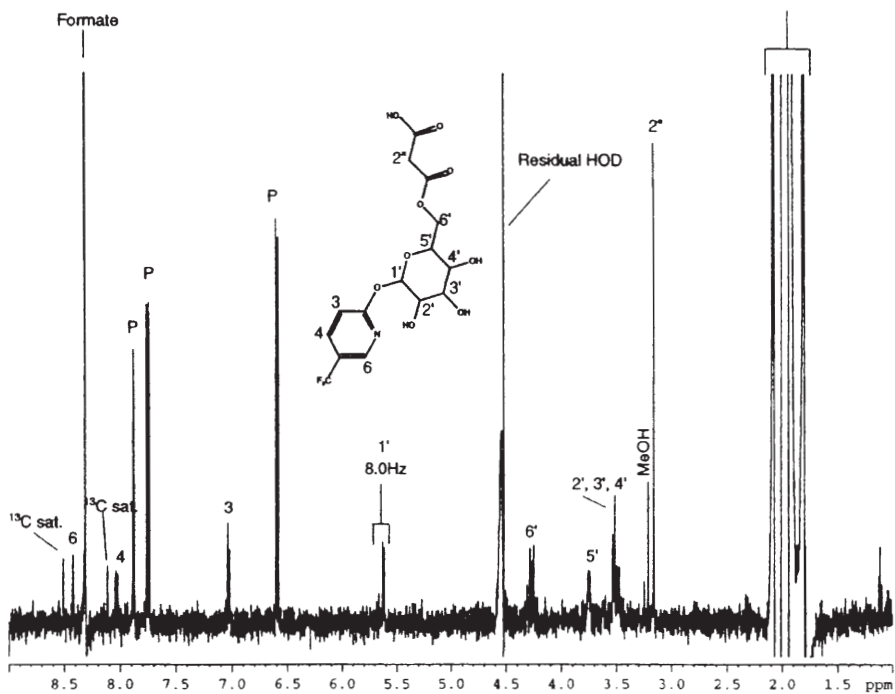
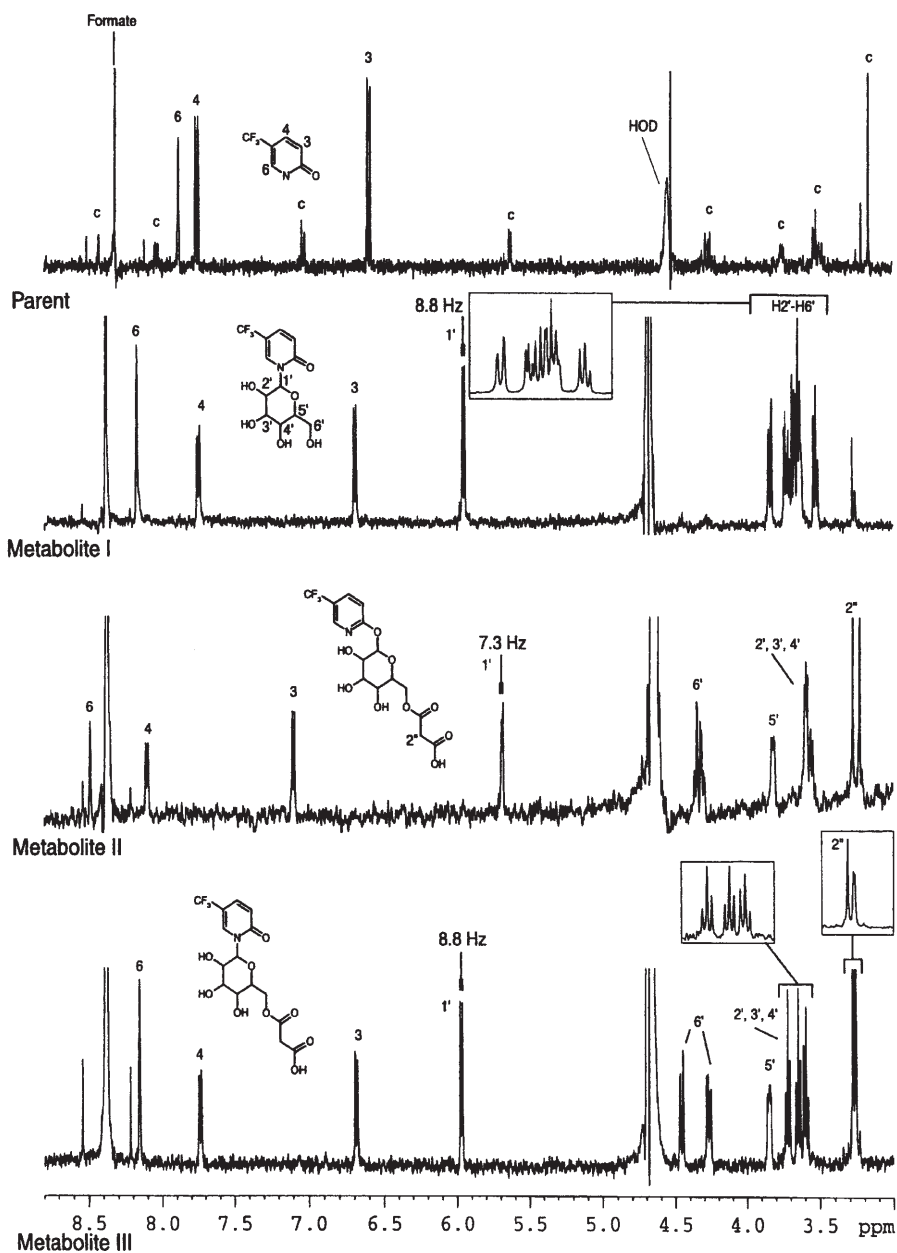


Fig. 18. UV detected HPLC chromatogram of maize extract after dosing with 5TMP. Metabolite peaks are indicated at 33.9 and 43.3 min (two co-eluting peaks). Reproduced with permission from J Agric Food Chem (2000) 48(1):42-46, Copyright (2000) American Chemical Society



**Fig. 19.** Stopped-flow 500 MHz  $^1\text{H}$  detected HPLC chromatogram of (from bottom to top): metabolite I, metabolite II contaminated with 5TFMP. Reproduced with permission from J Agric Food Chem (2000) 48(1):42–46, Copyright (2000) American Chemical Society



**Fig. 20.** Stopped-flow 500 MHz <sup>1</sup>H detected HPLC chromatogram of (from bottom to top): metabolite III, metabolite II, metabolite I and 5TFMP

tained in an LC peak with a retention time of 33 min, and that “Metabolite II” and 5TFMP co-elute in an LC peak eluting at 43 min. These findings can be transposed onto the complex UV chromatogram of the maize extract shown in (Fig. 18).

Using this information, the stopped flow 1D  $^1\text{H}$  NMR spectra (Brüker DRX 500) from the chromatography peaks identified above are shown in (Fig. 19). From these spectra it is possible to assign the chemical structure 5TFMP-*N*-glucoside to Metabolite I, and 5TFMP-*O*-6-malonylglucoside to Metabolite II. Since Metabolite II co-elutes with 5TFMP, signals from the latter are clearly observed in the  $^1\text{H}$  NMR spectrum, but the difference in molar concentration between the two components does not lead to confusion during the data interpretation step.

Coupled with a modification to the chromatography conditions, stopped-flow  $^{19}\text{F}$  NMR detected HPLC (Brüker DRX 500) enabled the detection of a signal for the low abundance Metabolite III and a partial separation of the other metabolite containing peak now eluting at 39 min. Stopped flow 1D  $^1\text{H}$  NMR spectra (Brüker DRX 500) of the identified chromatography peaks are shown in Fig. 20. From the spectrum of the newly identified  $^{19}\text{F}$ -containing chromatography peak it is possible to assign the chemical structure 5TFMP-*N*-6-malonylglucoside to Metabolite III. “Time-slicing”, i.e. advancing the chromatograph flow slowly through a peak and acquiring NMR spectra at each stopping point, allows the homogeneity of chromatography peaks to be investigated. “Time-slicing” through the chromatography peaks with retention times of approximately 39 min enables the acquisition of a spectrum of pure Metabolite II and of a slightly contaminated 5TFMP. In all these spectra, the approximate mass of material detected in the NMR probe was in the order of 5–10  $\mu\text{g}$ .

A second novel application of  $^{19}\text{F}$  NMR detected LC-NMR has been reported by Nicholson et al. [97] in which the acyl migration reaction of drug 1-*O*-acyl glucuronides is monitored. This reaction is of significance because of the possible role of acyl glucuronides in covalent binding to serum proteins and consequent allergic reactions.

## 2.3

### Quantitation of Metabolites

The registration of a chemical substance for use as a pesticide is preceded by many detailed studies that ensure the substance does not accumulate in crop species and that the substance and its metabolites do not have toxic, or adverse ecological, properties. The first step in this process is to identify the metabolites.

Such studies are normally carried out using  $^{14}\text{C}$  labelled materials, whereby the putative metabolites are located using thin layer chromatography (autoradiogram) or liquid chromatography and radiochemical detection. The isolation procedure for the metabolites, prior to spectroscopic structure elucidation, is time-consuming and often entails complex extraction procedures. When the substances are fluorinated,  $^{19}\text{F}$  NMR can often be used to advantage in addressing the problem; often, little or no clean up of the crude plant extracts is required. Normally this approach is only viable when the final concentration of

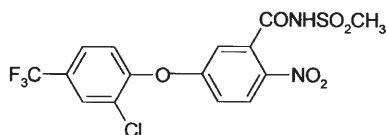
analytes is projected to be at levels greater than 1–5  $\mu\text{mol/l}$ . It should be emphasised that this concentration will normally only be achieved following reduction of a much larger extraction volume. Such quantities are compatible with the application rates and legislative detection limits for the registration of the current generation of herbicidally active compounds. The detection limit for each analyte is derived from a combination of the measured sensitivity of the available NMR spectrometer coupled with a sensible total acquisition time for each analysis and will be variable dependant upon the nature of the fluorine reporter group. For variously configured NMR instruments in the 270–500 MHz range, an accumulation time of 4 h will detect the  $^{19}\text{F}$  NMR signal from around 0.5  $\mu\text{g}$  of a  $\text{CF}_3$  substituted analyte (MW 300 Da) dissolved in 0.5 ml of NMR solvent. Using these guidelines, the concentration of the extracts from 25 g of crop material or 1L of groundwater to 0.5 ml will deliver, respectively, detection limits of 20 ppb following a 4 h accumulation time and 1 ppb following a 1-h accumulation time.

In our laboratory, we have used such principles to establish validated experimental protocols to detect residues and metabolites of a range of fluorine containing pesticides. In particular they have been used to support the registration of the herbicidally active substances fomesafen and fluazifop-butyl, the chemical structures of which are shown in Table 8.

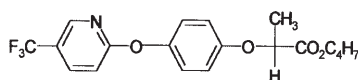
The comparative detection of fluorinated xenobiotics and their metabolites by both  $^{19}\text{F}$  NMR and  $^{14}\text{C}$  labelling techniques is discussed in the paper by Serre et al. [93]. Apart from an identification strategy for unknown fluorinated metabolites, this reference discusses the procedure required to acquire quantitative NMR data that deliver an equivalent sensitivity to the  $^{14}\text{C}$  method. To obtain reliable quantitative results ( $\pm 10\%$ ) the  $T_1$  relaxation rates of the analytes must be determined with some precision [19], since they will determine the cycle time for each separate NMR acquisition as they are summed, over several hours, to give the required detection limit.

It is tempting to set up the NMR acquisition so as to use conditions that deliver maximum sensitivity *per pulse*; i.e. a  $\pi/2$  ( $90^\circ$ ) pulse duration with a relaxation delay five times the  $T_1$  of the slowest relaxing analyte. However, for long-term data acquisition, using conditions that deliver the maximum sensitivity *per unit time* is preferable. The NMR pulse duration and relaxation time are related by the Ernst angle condition [37]. Under this condition, reducing the pulse

**Table 8.** Fomesafen and fluazifop-butyl



fomesafen: 5-[2-chloro-4-(trifluoromethyl)phenoxy]-*N*-(methylsulphonyl)-2-nitrobenzamide



fluazifop-butyl: 2-[4-[[5-(trifluoromethyl)-2-pyridinyl]oxy]phenoxy]propanoic acid, butyl ester

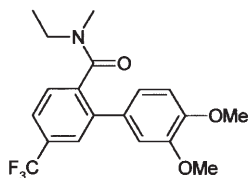
duration (e.g. to  $30^\circ$ ) allows the relaxation delay to be shortened whilst retaining the quantitative nature of the derived NMR data. Accordingly the 4 s cycle time of the maximum sensitivity *per pulse* condition can be reduced to 0.3 s by adopting the maximum sensitivity *per unit time* conditions specified by the Ernst condition. The summation of many more of these less sensitive pulses is a more effective strategy, on a per time basis, than the summation of fewer more sensitive pulses. In this case, by using the Ernst angle conditions and a total acquisition time of 4 h, the signal to noise ratio of the spectra were increased by a factor of 1.26 over the maximum sensitivity *per pulse* conditions.

In such cases the  $^{19}\text{F}$  NMR signals are very small and the acquisition conditions for the NMR spectrometer need to be set up with care. As discussed earlier, some NMR probes capable of  $^{19}\text{F}$  detection have a broad background  $^{19}\text{F}$  signal as a consequence of their manufacturing processes. During the collection of the time-domain NMR spectrum, the signal representing this broad baseline artefact will dominate the first few ( $n$ ) points of the FID. As a consequence, the acquisition conditions for the sample will be imperfectly set, resulting in a less than optimum detection of these small signals. NMR acquisition software normally allows adjustment of the data acquisition conditions so that the first  $n$  points of the FID can be omitted. Under these conditions, the instrument will adjust the acquisition parameters to collect data based on the signals present rather than those from the artefact peak, the missing data points being re-inserted using post-acquisition backward linear prediction.

Following acquisition of NMR data under quantitative conditions, the areas of the detected NMR peaks must be measured (*integrated*) to determine the concentration, and thus the mass, of each species present. Although it is possible to compare the relative amounts of material present in a series of NMR spectra from inspection of the instrumental parameters alone, this comparison is most often achieved by the addition of a “spike” of known substance to each analytical sample. The spike will normally have a  $^{19}\text{F}$  chemical shift close to that of the other analytes and can be used both as a chemical shift reference and a quantification standard.

The manual, or automatic, integration of the data typically produced from these analyses is not generally easy to perform with any accuracy. Deconvolution of the spectra using the curve fitting routines that form part of the basic functionality of most NMR spectrometer software often produces accurate and reproducible results where manual integration fails. In their paper

**Table 9.** Model fungicide



*N*-Ethyl-*N*-methyl-4-(trifluoromethyl)-2-(3,4-dimethoxyphenyl)benzamide

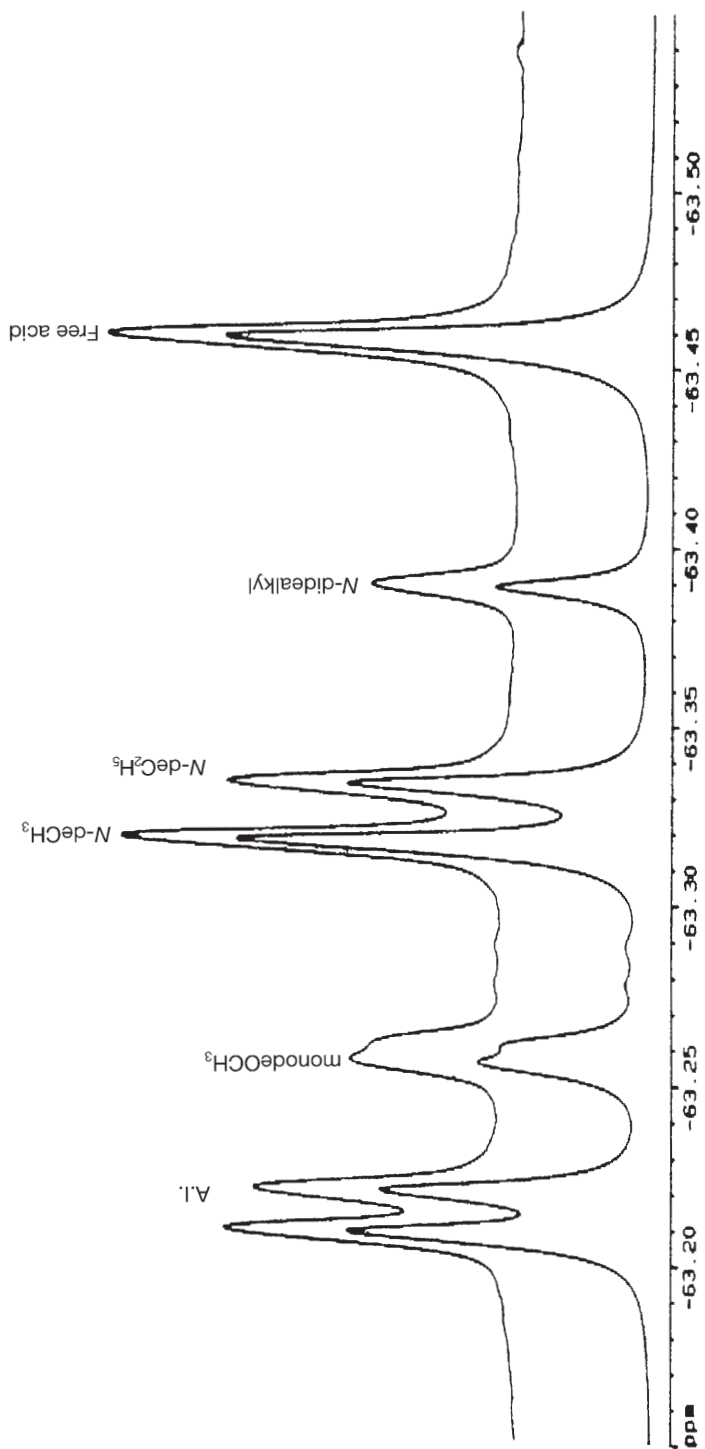


**Fig. 21.** The  $^{19}\text{F}$  NMR spectrum of fungicide model and related compounds, mixed at different concentrations in  $\text{CHCl}_3$ . The upper trace shows the experimental spectrum of model and five of its metabolites at different concentrations. The lower trace shows the calculated deconvolution of the experimental spectrum. Reproduced with permission from *J Agric Food Chem* (1997) 45(1):242–248, Copyright (1997) American Chemical Society

Serre et al. [93] discuss the identification and quantification of the metabolites of a model fungicide *N*-ethyl-*N*-methyl-4-(trifluoromethyl)-2-(3,4-dimethoxyphenyl)benzamide, shown in (Table 9).

The efficiency of the deconvolution method is shown in (Fig. 21), in which the upper trace shows the experimental spectrum of the model fungicide (labelled AI) and five of its metabolites that were added at different concentrations.

The lower trace shows the calculated deconvolution of the experimental spectrum. The concentrations of the various components were calculated from the deconvolution data with  $\text{CFCl}_3$  (1 mmol/l) as a reference. From left to right the results are as follows: AI 2.57 mmol/l calculated concentration/2.50 mmol/l actual concentration; 3-mono-de $\text{OCH}_3$ , 1.25/1.25 mmol/l; *N*-de $\text{CH}_3$ , 1.84/1.88 mmol/l; *N*-de $\text{C}_2\text{H}_5$ , 1.31/1.25; *N*-didealkyl, 0.68/0.62 mmol/l; free acid, 2.33/2.50 mmol/l.

Other applications in this area include a comparison of  $^{19}\text{F}$  NMR and GC-ECD for analysing trifluralin residues in field grown crops [69], the  $^{19}\text{F}$  NMR analysis of trifluralin in a range of crops and derivative products [70] and the generic detection of  $\text{CF}_3$ -containing residues at or near the legislative tolerance levels in foodstuffs [63]. Applications to animal systems include an investigation of the toxic effects of 3-trifluoromethylaniline on earthworms [108] and the quantification of the metabolites of 2,3,5,6-tetrafluoro-4-trifluoromethylaniline by using  $^{19}\text{F}$  NMR as a part of a strategy incorporating a range of hyphenated techniques [90].

## 2.4

### Solid State NMR Applications

#### 2.4.1

##### Gels

A detailed discussion of the theory of the NMR of solid samples is beyond the scope of this chapter. With reference to NMR spectroscopy, the difference between the liquid and the solid state is the timescale and geometry of molecular motion. In liquid samples the intramolecular effects – dipolar coupling, quadrupolar interactions and chemical shift anisotropy – are averaged to zero by rapid molecular motion. In solid samples intramolecular effects are pronounced and the NMR spectrum of a typical solid sample consists of broad overlapping signals whose widths and shapes provide information about molecular motion within the sample as well as giving the distribution of particular molecular orientations within an ordered sample.

In semi-solid samples there is sometimes sufficient molecular motion to give useable NMR spectra. The NMR spectra of “gel-phase” samples such as swollen solid phase beads inserted into a conventional NMR tube are a case in point. For such samples, proton NMR is usually uninformative but Shapiro and Wareing [95] point out that  $^{19}\text{F}$  NMR is particularly useful because of its large chemical shift range and because structural modifications quite remote from the fluorine can give rise to useful chemical shift changes [104]. High quality  $^{19}\text{F}$  NMR spectra can be obtained from substances bonded to 20–500 mg of TentaGel resin in a very short time, in which the spectral line-widths are almost the same as in

solution. Accordingly chemical shift differences of 0.5 ppm can be readily distinguished. A large variety of fluorine-containing building blocks and reagents are commercially available, allowing the use of fluorine as a convenient reporter for gel-phase chemistry without the need to resort to the synthesis of special materials. Gel-phase  $^{19}\text{F}$  NMR has been used successfully to monitor nucleophilic aromatic substitution reactions [94].

### 2.4.2

#### ***Semi-Solids***

For true solid samples, even  $^{19}\text{F}$  spectra are often too broad to be useful. Several techniques have been developed to overcome the problem of the spectrum broadening encountered in solid samples. In principle, the broadening can be removed by imitating the motions of molecules in a liquid. To a good approximation, all the intermolecular broadening effects are proportional to  $(3 \cos^2 \theta - 1)$ , where  $\theta$  is the angle between the coupling vector of two spins and the magnetic field. This term reduces to zero when  $\theta = 54.7^\circ$ , the “magic angle”. If the entire sample is rotated at this angle, within the magnetic field of the NMR spectrometer, with a rotational frequency greater than the frequency range of the interaction the effects of the interactions are removed from the spectrum. This technique is known as magic angle spinning (MAS).

In semi-solid samples, such as tissue samples and those polystyrene beads with shorter linkers than TentaGel some components of a “solid” sample will still have reasonable molecular motion. This motion may well be slower or more hindered than in solution and may be anisotropic, resulting in moderate line broadening due to residual dipolar interactions and sample heterogeneity. Rapid spinning of the sample, typically 2–15 kHz, at the magic angle is often sufficient to significantly reduce or eliminate the broadening experienced by the more mobile components in the sample. The improvement in sensitivity and resolution obtained can be quite dramatic. It should be noted that this does not involve the use of high-power decoupling or any of the special techniques commonly used to obtain NMR spectra from true solids. To distinguish it from true solid state NMR, the technique has been dubbed “high-resolution magic angle spinning” (HR-MAS). In our laboratory we have successfully used a Varian Nano-NMR probe to observe  $^{19}\text{F}$  spectra from a range of semi-solid samples. The same type of equipment was used to generate the NMR data used to quantitate reaction products of solid phase synthesis [33]. The best quality spectra were obtained from samples consisting of 2–4 mg of resin swollen with DMF; spinning speed was in the range 1.5–1.7 kHz.

### 2.4.3

#### ***Solids***

True solids require the higher spin rates that are only obtainable from purpose build MAS probes, which typically spin samples at up to 20 kHz.  $^{19}\text{F}$  solid state NMR was used to investigate the sorption of hexafluorobenzene to soil organic matter [59]. The authors demonstrated that the sorptive uptake of hexafluoro-

robenzene gives direct spectroscopic evidence for the existence of dual-mode sorption to soil organic matter. The sorption process was shown to be rapid, with all the applied hexafluorobenzene being adsorbed within a few hours. Extractable lipids competed for high-energy sorption sites in the organic matter, and their removal increased the amount of rigidly sorbed immobile species present. Soil lipids enhance the sorption capacity of the solid-state dissolution domain of the organic matter and this dissolution domain was responsible for partitioning in the dual-mode phenomenon. Removing the lipids decreased the partitioning capacity of the soil organic matter. A second paper [28] describes the use of  $^{19}\text{F}$  NMR to probe the mechanism of sorption in a range of sediments and polymers.

## 2.5

### Biochemical Studies

#### 2.5.1

##### *Labels and Tags*

Since fluorine is infrequent as a substituent in naturally occurring substances (covered elsewhere in this volume) and is generally resistant to degradation, once incorporated into a biological substrate it functions as an indelible label that, with minimal background interference, can be used to monitor biochemical structure and dynamics in solution using spectroscopic methods. The intrinsic low sensitivity of the NMR experiment persistently limits the generic applicability of NMR techniques to biochemical systems: whereas NMR measurements are most often made at millimolar concentrations, many relevant biochemicals are only present at sub-micromolar levels. Although advances in technology are gradually improving the sensitivity of NMR instruments, this threefold order of magnitude deficit in abundance will remain a real challenge for the foreseeable future. Within limits, it is possible to increase the detectability of fluorinated substances by increasing the fluorine content of the label. For example the signal intensity of a trifluoroacetyl substituent, a commonly used reporter substituent for amino acids, carbohydrates and steroids has three times the sensitivity of a monofluoro derivative.

The review by Everett [38], cited in Sect. 1.6, contains a comprehensive list of references that exemplify the ways in which  $^{19}\text{F}$  NMR has been used as a biochemical probe.

Some more recent novel applications include the determination of the antioxidant capacity of bio-molecules using high resolution  $^{19}\text{F}$  NMR [4]. This method is based on the use of trifluoroacetylated reporters such as trifluoroacetanilide. Upon hydroxyl radical attack such fluorinated detectors yield trifluoroacetamide and trifluoroacetic acid that can be quantitatively determined by  $^{19}\text{F}$  NMR.

Both 1D and 2D  $^{19}\text{F}$  NMR methods have been used to determine the conformational heterogeneity of modified DNA fragments [113]. The real-time refolding of 6-fluoro-tryptophan labelled proteins have been monitored using stopped-flow  $^{19}\text{F}$  NMR [48].

### 2.5.2

#### **Magnetic Resonance Imaging (MRI)**

MRI is a non-invasive diagnostic technique commonly used in both medicine and materials science. A readily understandable guide the principle of MRI is to be found at Hornak's website [50]. Using MRI techniques it is possible to measure a number of chemical and physical parameters, temporally and spatially resolved, in intact biological systems. Since MRI measurements do not perturb the metabolic and transport processes within organisms, mediation of these processes brought about by a change in environment and in response to a chemical challenge can be observed particularly well. Fluorine MRI is a relatively new technique and has been used clinically to investigate the oxygenation of tumours [64] and many dynamic processes such as cerebral oxygen consumption and blood flow [79]. MRI techniques have also been used extensively in materials science. In addition to normal imaging methodologies, the less well-known stray field imaging (STRAFI) technique enables NMR images to be generated using the large magnetic field gradients that occur *outside* a normal NMR magnet. Dental cements [60] and solid paramagnetic species [83] have both been studied using  $^{19}\text{F}$  STRAFI methods.

### 2.5.3

#### **Drug Design**

In drug or other “effect chemicals” design, ligand binding by a target protein induces the ultimate effect of interest, such as cell growth or cell death. With knowledge of the structure of the protein targeted by a particular disease state and its relevant ligand binding sites it may be possible to design inhibitors or activators to fit the architecture and chemical nature of that site and to elicit the desired response.

To observe ligand binding in solution, the NMR spectrum of ligand-free protein is compared with that of the ligand-bound protein. When a ligand binds to a protein, the NMR signals from amino acid residues in, or close to, the binding site may move, broaden or disappear. To ensure that binding is occurring at the site of interest, it is essential to have access to the spectroscopic assignment of signals from the amino acids that form that binding site. The total assignment of the NMR spectra of proteins is a task not to be undertaken lightly since both data acquisition and analysis involve complex procedures. To speed up the acquisition of the spectroscopic data it is preferable to use labelled proteins whenever they are available. With proteins having molecular weights greater than around 7 kDa,  $^{15}\text{N}$  incorporation is generally sufficient; proteins with molecular weights greater than 15 kDa generally require both  $^{15}\text{N}$  and  $^{13}\text{C}$  labelled material; when the molecular weight is greater than 25 kDa it is preferable to use  $^{15}\text{N}$ ,  $^{13}\text{C}$ ,  $^2\text{H}$  triply labelled substrates. Measuring changes in chemical shifts and hydrogen exchange rates serves to elucidate the dynamics of ligand binding and determines the critical residues for ligand-protein interactions [101].

The landmark paper by Fesik et al. [96] describes how NMR may play a directive role in the process of discovering which ligands bind effectively to a spe-

cific protein thereby making a significant contribution to the process of discovering new active substances. This elegant method has become known as “SAR by NMR” (structure/activity relationships by NMR) and neatly spans the paradigm of rational design and high throughput screening strategies by applying mixtures of carefully chosen small molecules (ligands) to the target protein. The resulting [ $^{15}\text{N}$ ] HSQC spectra are capable of detecting ligand-protein bindings that are below the level of detection of conventional *in vitro* biochemical assays. After finding small molecules that bind, albeit weakly, at different yet proximal sites in the protein the two molecules can be linked together in the proper orientation to produce a tightly binding, and thus more potent, substance. At a recent conference it was revealed that this methodology and subsequent developments produce almost 20% of all lead substances within the author’s business.

This immensely powerful method is relatively input intensive since it requires a backbone assignment of the target protein and a supply of  $^{15}\text{N}$  labelled material. This method has also been subjected to patent protection, which has no doubt played some part in the spawning of several related proton NMR and mass spectrometry [47, 88] based methods.

These alternative NMR methods are based on either a single measurement or combination of NOE [67, 86], molecular translational motion [25] (diffusion) and NMR line-shape measurements [68]. All these methods share the common advantage that they measure changes in the ligand signal rather than the protein; therefore neither the complete spectrum assignment of the protein nor labelled material is required. The disadvantage of these methods is that there is no guarantee that the measurements are related to the binding site of interest. In principle all these processes can be observed using  $^{19}\text{F}$  NMR provided the ligands contain fluorine as either an essential constituent or as a tag. The 1991 review article by Jenkins [54] describes the study of ligand-macromolecular interactions monitored by  $^{19}\text{F}$  NMR. The review covers the determination of protein/ligand equilibrium constants and stoichiometries, the co-binding and competition of ligands, allosteric and conformational effects together with reaction kinetics. Chemical models include the interaction of 5-fluorotryptophan, 5-fluorosalicic acid, flurbiprofen and sulindac sulfide with human serum albumin.

## 2.6

### Determination of Optical Purity – Fluorinated Derivatisation Reagents

For any chemical structure, the determination of the absolute stereochemistry is vital for a complete understanding of its chemical and biochemical reactions. Many chemists apply a mixture of degradative chemistry, total synthesis and X-ray analysis as the arbiter between similar working structures. In addition to X-ray analysis, optical rotatory dispersion (ORD) and circular dichroism (CD) are effective techniques providing that a chromophore is present. Many empirical methods exist to determine absolute stereochemistry, amongst them NMR. The NMR spectra of enantiomers of a chemical structure are identical, whereas the NMR spectra of diastereomers are potentially different.

There are three ways of using this methodology to investigate the optical purity of substances, and hence make inferences about their absolute stereochemistry. All methods rely on inducing diastereoisomerism in an optically pure material by chemical reaction or complexation. The high sensitivity and wide chemical shift range of  $^{19}\text{F}$  nuclei make it the ideal tool to monitor these processes, either when  $^{19}\text{F}$  is present in the substance or when it can be introduced as part of a derivatisation process. The separate  $^{19}\text{F}$  signals from these diastereoisomeric derivatives can be identified and quantified, thus determining the optical properties of the original compound. It should be born in mind, however, that the  $^{19}\text{F}$  chemical shift differences between diastereoisomers are often small (less than 1 ppm). Although this limits the technique, especially when the  $^{19}\text{F}$  signal is extensively coupled, the resulting spectra are almost always easier to work with than the complex spectra derived from proton NMR. Analysis based on  $^{19}\text{F}$  NMR does not of course preclude the use of the proton spectrum when  $^{19}\text{F}$  chemical shifts are not diagnostic. Although quite old, the volume by Martin et al. [62] still serves as a useful source of practical information on the use of NMR methods to assess optical purity. A more recent review [17] discusses the preparation and properties of chiral organofluorine substances with respect to the reaction of chiral reagents with prochiral fluorinated substrates.

Chemical derivatisation is often not the method of choice since it involves an additional step prior to analysis, and it can introduce uncertainties arising from the mechanism of the reaction. Many references, however, report the successful application of this approach and a wide range of suitably pure derivatising reagents are available commercially: these include  $\alpha$ -methoxy- $\alpha$ -trifluoromethylphenylacetic acid (MTPA or Mosher's acid) [30], 2,2,2-trifluoro-1-(9-anthryl)ethanol (Pirkel's reagent) [82] and 1-amino-2-fluoro-2-phenylethane [46]. Classes of compounds that may be analysed using this methodology include alcohols, amines and carboxylic acids. Reliance on amide formation to induce diastereoisomerism can be equivocal since rotation of amide bonds often results in the existence of two forms that are in dynamic equilibrium, and that are resolvable under the conditions of the NMR experiment.

If it is desired to avoid chemical derivatisation, the use of either chiral lanthanide shift reagents or "chiral solvents" should be considered. Chiral lanthanide shift reagents are appropriate when the substrate contains basic functional groups capable of co-ordinating with a metal. Increased effectiveness is to be expected when the co-ordinating site in the substrate is close to the chiral centre. As for any lanthanide shift reagent, scrupulous laboratory techniques are required to guarantee success and reproducibility; these techniques are described in the volume by Martin et al. referred to above.

Chiral lanthanide shift reagents may generically be represented as  $(\text{L})_3\text{M}(\text{III})$ , where L represents a chiral ligand and M a paramagnetic metal from the lanthanide series. A representative selection of the reagents that are available commercially uses either 3-trifluoromethylhydroxymethylene-*d*-camphor (facam), 3-heptafluoropropylhydroxymethylene-*d*-camphor (hfbc) or *d,d*-dicampholylmethane (dcm) as the ligand, and either europium or praseodymium as the paramagnetic metal. When the resultant diastereoisomeric complexes have the

same geometry, europium and praseodymium induce chemical shift changes in the substrate that are in opposite directions. Chiral shift reagents do not, however, work well in aqueous conditions, and for compounds with sufficient water solubility, the measurement of NMR spectra following complexation with cyclodextrins should be considered [44].

### 3 Conclusions and a Prospective View

The aim of this chapter has been to give an overview of the relevance of fluorine as a sensitive probe of chemical structure and to illustrate how the rarity of fluorine, as a naturally occurring substituent, in organic substances can be used to advantage in locating and quantifying significant products of chemical reactions and metabolic processes.

The high intrinsic NMR sensitivity of  $^{19}\text{F}$  coupled with its wide spectral range means that informative  $^{19}\text{F}$  NMR data can be obtained using NMR spectrometers with the most modest performance, often with no modification of the basic hardware. It is even possible to identify various fluorinated residues *without actually performing  $^{19}\text{F}$  NMR* [26]. This interesting procedure relies on the pictorial analysis of the contour patterns formed within the correlation islands of 2D  $^{13}\text{C}/^1\text{H}$  correlation spectra. Using this method, the identification of the position of fluorination in a substance can be inferred relatively simply and, additionally, allows other significant NMR parameters (e.g.  $^{19}\text{F}/^{13}\text{C}$  and  $^{19}\text{F}/^1\text{H}$  spin-spin coupling constants) can be obtained directly from the plots.

As pointed out several times throughout this chapter, the sensitivity of the NMR experiment is rather low compared to other spectroscopic techniques and the optimisation of NMR sensitivity has almost become a research topic in its own right. There are several possibilities for increasing the signal-to-noise ratio (S/N) of NMR spectra [45]:

1. Increase the static magnetic field ( $B_0$ )
2. Increase the sample concentration within the detector coil
3. Increase the sample and coil volume when the solubility of the sample is limited
4. Reduce the sample coil volume when the amount of substance is limited
5. Increase the number of transients acquired
6. Choose the most sensitive nuclear species for excitation and detection
7. Use pulse sequences optimised for the molecular weight of interest [76]

A different, purely electronic, approach for increasing NMR S/N is to reduce thermal noise within the signal pathway of the NMR spectrometer by cooling them to extremely low temperatures [71]. The first commercial cryogenic probes configured for either dual frequency or inverse triple resonance experiments were introduced by Brüker in 1999. In these devices both the receiver coil and the signal preamplifier are cooled to low temperatures with helium gas. The spatial requirements for insulating and cooling the coil result in a reduction of the probe filling factor and the absolute signal amplitude generated. Even so, the reduction in noise with these cryogenic NMR probes dominates and there is a

significant increase in S/N per transient compared with the results obtained from an equivalent conventional probe.

The comparison of the performance of a cryogenic and conventional probe is described in the paper by Martin [87]. Using a 3-mm cryogenic probe from another manufacturer (Nalorac), the acquisition of the HSQC spectrum from a small strychnine standard afforded a 12- to 16-fold reduction in data acquisition time for a comparable S/N ratio spectrum.

Although the present major area of development for the manufacturers of these probes is to optimise inverse triple resonance performance for use in protein studies,  $^{19}\text{F}$  detection probes have been constructed that offer the 3- to 4-fold sensitivity gains expected from theory. Using such devices will push the level of detection of suitable fluorinated materials into the low nanogram range using acceptable acquisition times.

The commercial significance of fluorinated materials, coupled with the favourable NMR properties of  $^{19}\text{F}$  nuclei, resulted in an enormous amount of historical literature focused on  $^{19}\text{F}$  NMR principles and practice. At one time relegated to a confirmational tool, access to modern NMR instrumentation and pulse methods have revitalised the technique as a tool for chemical structure elucidation and quantitative analysis. The many new applications appearing in the current literature indicate that  $^{19}\text{F}$  NMR will continue to be used appropriately as a powerful member of the armoury of modern analytical techniques.

## 4 Appendix

IUPAC guidelines for the acquisition and reporting of  $^{19}\text{F}$  NMR data are:

1. Use fluorotrichloromethane ( $\text{CCl}_3\text{F}$ ) as the standard reference.
2. Use the standard sign convention of (+) for signals downfield from (left of)  $\text{CCl}_3\text{F}$  and (-) for signals upfield from (right of)  $\text{CCl}_3\text{F}$ . The vast majority of C-F signals are negative.
3. Give a clear indication of solvent, concentration and temperature. These parameters have a much greater effect on chemical shifts and coupling constants for fluorine than for protons.
4. Give an exact description of instrumentation – magnetic field strength, pulse sequence, decoupling mode etc.
5. Use standardised plotting and spectral presentations, comparable to  $\delta$  0–10 used for proton spectra. The range from  $\delta$  +50 to -250 covers most organofluorine signals but is too wide to show small spin-spin couplings. To measure spin-spin couplings accurately it is usual to re-acquire the particular areas of interest with higher digital resolution.

## 5 References

1. Advanced Chemistry Development Inc, Toronto, Canada ACD/CombiNMR, [http //www acdlabs com/](http://www.acdlabs.com/)
2. Advanced Chemistry Development Inc, Toronto, Canada ACD/Structure Elucidator, [http //www acdlabs com/](http://www.acdlabs.com/)
3. Advanced Chemistry Development Inc, Toronto, Canada [http//www acdlabs com/](http://www.acdlabs.com/)
4. Aime S, Calzoni S, Digilio G, Giraudo S, Fasano M, Maffeo D (1999) A novel  $^{19}\text{F}$ -NMR method for the investigation of the antioxidant capacity of biomolecules and biofluids. *Free Radical Biol Med* 27(3/4):356–363
5. Aue WP, Bartholdi E, Ernst RR (1975) Two-dimensional spectroscopy; application to nuclear magnetic resonance. *J Chem Phys* 64(5):2229–2246
6. Bailey NJC, Cooper P, Hadfield ST, Lenz EM, Lindon JC, Nicholson JK, Stanley PD, Wilson ID, Wright B, Taylor SD (2000) Application of directly coupled HPLC-NMR-MS/MS to the identification of metabolites of 5-trifluoromethylpyridone (2-hydroxy-5-trifluoromethylpyridine) in hydroponically grown plants. *J Agric Food Chem* 48(1):42–46
7. Bax A, Summers MF (1986) Proton and carbon-13 assignments from sensitivity-enhanced detection of heteronuclear multiple-bond connectivity by 2D multiple quantum NMR. *J Am Chem Soc* 108(8):2093–2094
8. Bayer E, Albert K, Nieder M, Grom E, Wolff G, Rindlisbacher M (1982) On-line coupling of liquid chromatography and high-field nuclear magnetic resonance spectrometry. *Anal Chem* 54(11):1747–1750
9. Bendall MR, Doddrell DM, Pegg DT (1981) Editing of carbon-13 NMR spectra. 1. A pulse sequence for the generation of subspectra. *J Am Chem Soc* 103(15):4603–4605
10. Benecke C, Grund R, Hohberger R, Kerber A, Laue R, Wieland T (1995) Molgen structure elucidation program from Chemical Concepts
11. Bigler P (1997) NMR spectroscopy processing strategies. VCH
12. Bladon P (2000) Personal communication to The NMR Newsletter
13. Bodenhausen G, Ruben DJ (1980) Natural abundance nitrogen-15 NMR by enhanced heteronuclear spectroscopy. *Chem Phys Lett* 69(1):185–188
14. Bothner-By AA, Stephens RL, Lee, J-M, Warren CD, Jeanloz RW (1984) Structure determination of a tetrasaccharide: transient nuclear Overhauser effects in the rotating frame *J Am Chem Soc* 106(3):811–813
15. Braun S, Kalinowski H-O, Berger S (1999) 150 and more basic NMR experiments. VCH
16. Braunschweiler L, Ernst RR (1983) Coherence transfer by isotropic mixing: application to proton correlation spectroscopy. *J Magn Reson* 53(3):521–528
17. Bravo P, Resnati G (1990) Preparation and properties of chiral fluoroorganic compounds. *Tetrahedron Asym* 1 (10):661–692
18. Bremser W (1978) HOSE – a novel substructure code. *Anal Chim Acta* 103(4):355–365
19. Canet D, Levy GC, Peat IR (1975) Time saving in  $^{13}\text{C}$  spin-lattice relaxation measurements by inversion recovery. *J Mag Reson* 18:199–204
20. Carpenter KA, Reynolds WF, Yang JP, Enriquez RG (1992) Further improvements in the FLOCK sequence. *Mag Reson Chem* 30:S35–S41
21. Cavalli L (1976) *Annu Rep NMR Spectrosc* 6B:43
22. Chapman JR (1995) *Practical Organic mass spectrometry – a guide for chemical and biochemical analysis*. Wiley
23. Cheatham S, Adams B, Kupce E (1999)  $^{19}\text{F}$  decoupling. *Mag Moments* 10(1):1–8
24. Chemical Concepts SpecInfo [http//www chemicalconcepts com/](http://www.chemicalconcepts.com/)
25. Chen A, Shapiro MJ (1999) Affinity NMR. *Anal Chem News Feat* Oct 1:669–675
26. Cholli AL (1991) Pattern recognition in 2D NMR contour maps for studying molecules containing fluorines. Part I: Study of organofluorine ethers. *Appl Spectrosc* 45(5):839–848
27. Claridge TDW (1999) *High resolution NMR techniques in organic chemistry*. Pergamon

28. Cornelissen G, Van Noort PCM, Nachtegaal G, Kentgens APM (2000) A solid-state fluorine-NMR study on hexafluorobenzene sorbed by sediments, polymers and active carbon. *Environ Sci Technol* 34(4):645–649
29. Crews P, Rodríguez J, Jaspars M (1998) *Organic structure analysis*. Oxford
30. Dale JA, Dull DL, Mosher HS (1969)  $\alpha$ -Methoxy- $\alpha$ -trifluoromethylphenylacetic acid, a versatile reagent for the determination of enantiomeric composition of alcohols and amines *J Org Chem* 34(9):2543–2549
31. Derome AE (1987) *Modern NMR techniques for chemistry research*. Pergamon
32. Dorn HC (1984) Proton NMR: a new detector. *Anal Chem* 56(6):747A–758A
33. Drew M, Orton E, Krolikowski P, Salvino JM, Kumar NV (2000) A method for quantitation of solid-phase synthesis using  $^{19}\text{F}$  NMR spectroscopy. *J Comb Chem* 2(1):8–9
34. Dungan CH, Van Wazer JR (1970) *Compilation of reported  $^{19}\text{F}$  NMR chemical shifts 1951 to mid-1967*. Wiley-Interscience
35. Emsley JW, Phillips L (1971) *Prog Nucl Magn Reson Spectrosc* 7:1
36. Emsley JW, Phillips L, Wray V (1976) *Prog Nucl Magn Reson Spectrosc* 10:83
37. Ernst RR, Anderson WA (1966) Application of Fourier transform spectroscopy to magnetic resonance. *Rev Sci Instrum* 37:93–102
38. Everett TS (1995) Nuclear magnetic resonance spectroscopy of organofluorine compounds. In: Hudlicky M (ed) *Chemistry of organic fluorine compounds 11*. ACS Monograph, vol 187, pp 1037–1086
39. Fields R (1977) *Annu Rep NMR Spectrosc* 7:1
40. Fields R (1972) *Annu Rep NMR Spectrosc* 5A:99
41. Foxall PJD, Parkinson JA, Sadler IH, Lindon JC, Nicholson JK (1993) Analysis of biological fluids using 600 MHz proton NMR spectroscopy: application of homonuclear two-dimensional J-resolved spectroscopy to urine and blood plasma for spectral simplification and assignment. *J Pharm Biomed Anal* 11(1):21–31
42. Freeman R, Morris GA (1978) Experimental chemical shift correlation maps in nuclear magnetic resonance spectroscopy. *J Chem Soc Chem Commun* 684–686
43. Ghuari FYK, Wilson ID, Nicholson JK (1990) Fluorine-19 and proton-NMR studies of the metabolism of 4-trifluoromethylbenzoic acid in the rat. *Methodol Surv Biochem Anal* 20:321–324
44. Greatbanks D, Pickford R (1987) Cyclodextrins as chiral complexing agents in water, and their application to optical purity measurements. *Magn Reson Chem* 25:208–215
45. Griesinger C, Schwalbe H, Schleucher J, Sattler M (1994) *Two-dimensional NMR spectroscopy*, 2nd edn. VCH, pp 457–580
46. Hamman SJ (1989) *J Fluorine Chem* 45:377
47. Heck AJR (1999) Ligand fishing by mass spectrometry. *Spectrosc Eur* 11:12–17
48. Hoeltzli SD, Frieden C (1996) Real-time refolding studies of 6- $^{19}\text{F}$ -tryptophan labeled *Escherichia coli* dihydrofolate reductase using stopped flow nmr spectroscopy. *Biochemistry* 35(51):16,843–16,851
49. Hore PJ (1995) *Oxford chemistry primers 32*. Oxford University Press
50. Hornak JP (1999) The basics of MRI <http://www.cis.rit.edu/htbooks/mri/inside.htm>
51. Hurd RE (1991) Gradient enhanced spectroscopy. *J Magn Reson* 87(2):422–428
52. Hwang T-L, Kadkhodaei M, Mohebbi, A Shaka AJ (1992) Coherent and incoherent magnetisation transfer in the rotating frame. *Magn Reson Chem* 30:S24–S34
53. Hwang T-L, Shaka AJ (1992) Cross relaxation without TOCSY: transverse rotating-frame Overhauser effect spectroscopy *J Am Chem Soc* 114(8):3157–3159
54. Jenkins BG (1991) Detection of site-specific binding and co-binding of ligands to macromolecules using  $^{19}\text{F}$  NMR. *Life Sci* 48:1227–1240
55. Jones K, Mooney EF (1970) *Annu Rep NMR Spectrosc* 3:261
56. Jones K, Mooney EF (1971) *Annu Rep NMR Spectrosc* 4:391
57. Kay LE, Keifer P, Saarinen T (1992) Pure absorption gradient enhanced heteronuclear single quantum correlation spectroscopy with improved sensitivity. *J Am Chem Soc* 114(26):10,663–10,665

58. Kessler H, Griesinger C, Zarbock J, Loosli HR (1984) Assignment of carbonyl carbons and sequence analysis in peptides by heteronuclear shift correlation via small coupling constants with broadband decoupling in t1 (COLOC). *J Magn Reson* 57(2):331–336
59. Kohl SD, Toscano PJ, Hou WH, Rice JA (2000) Solid-state  $^{19}\text{F}$  NMR investigation of hexafluorobenzene sorption to soil organic matter. *Environ Sci Technol* 34(1):204–210
60. Lloyd CH, Scrimgeour SN, Hunter G, Chudek JA, Lane DM, McDonald PJ (1999) Solid state spatially resolved  $^1\text{H}$  and  $^{19}\text{F}$  nuclear magnetic resonance spectroscopy of dental materials by stray field imaging. *J Mater Sci Mater Med* 10(6):369–373
61. Magnetic resonance microsensors. Savoy, Illinois USA
62. Martin ML, Delpeuch J-J, Martin GJ (1980) *Practical NMR Spectroscopy*. Heyden, pp 191–193
63. Mazzola EP, Borsetti AP, Page SW, Bristol DW (1984) Determination of pesticide residues in foods by fluorine-19 Fourier transform nuclear magnetic resonance spectroscopy. *J Agric Food Chem* 32(5):1102–1103
64. McIntyre DJO, McCoy CL, Griffiths JR (1999) Tumour oxygenation measurements by  $^{19}\text{F}$  magnetic resonance imaging of perfluorocarbons. *Curr Sci* 76(6):753–761
65. Mooney EF (1970) *Introduction to  $^{19}\text{F}$  NMR Spectroscopy*. Heyden
66. Mooney EF, Winson PH (1968) *Annu Rep NMR Spectrosc* 1:243
67. Moore JM (1999) NMR screening in drug discovery. *Curr Opin Biotechnol* 10:54–58
68. Moore JM (1999) NMR techniques for characterisation of ligand binding: utility for lead generation and optimization in drug discovery. *Peptides Sci* 151:221–243
69. Mortimer RD, Black DB, Dawson BA (1994) Pesticide residue analysis in foods by NMR. 3. Comparison of  $^{19}\text{F}$  NMR and GC-ECD for analysing trifluralin residues in field grown carrots. *J Agric Food Chem* 42(8):1713–1716
70. Mortimer RD, Dawson BA (1991) Using fluorine-19 NMR for trace analysis of fluorinated pesticides in food products. *J Agric Food Chem* 39(10):1781–1785
71. Moskau D, Richter C, Kovacs H, Salzmann M, Baselgia L, Haerberli M, Marek D, Schett O (2001) Highest sensitivity for cutting-edge NMR applications: 600 MHz CryoProbes. *Bruker Report* 149, pp 19–21
72. Neuhaus D, Williamson M (1989) The nuclear Overhauser effect in structural and conformational analysis. *VCH*, pp 217–240
73. Neuhaus D, Williamson M (1989) The nuclear Overhauser effect in structural and conformational analysis. *VCH*, pp 253–305
74. Nicholson JK, Wilson ID (1989) High resolution proton magnetic resonance spectroscopy of biological fluids. *Prog Nucl Magn Reson Spectrosc* 21(4/5):449–501
75. Olson DL, Lacey ME, Sweedler JV (1998) High-resolution microcoil NMR for analysis of mass-limited nanoliter samples. *Anal Chem* 70(3):645–650
76. Palmer AG III, Cavanagh J, Wright PE, Rance M (1991) Sensitivity improvement in proton-detected two-dimensional heteronuclear correlation NMR spectroscopy. *J Magn Reson* 93(1):151–170
77. Parella T, Sanchez-Ferrando F, Virgili A (1997) Improved sensitivity in gradient-based 1D and 2D multiplicity edited HSQC experiments. *J Magn Reson* 126(2):274–277
78. Patt S, Shoolery JN (1982) Attached proton test for carbon-13 NMR. *J Magn Reson* 46(3):535–539
79. Pekar J, Sinnwell T, Ligeti L, Chesnick AS, Frank JA, McLaughlin AC (1995) Simultaneous measurement of cerebral oxygen consumption and blood flow using  $^{17}\text{O}$  and  $^{19}\text{F}$  magnetic resonance imaging. *Cereb Blood Flow Metab* 15(2):312–20
80. Peng C, Yuan S, Zheng J (1994) Efficient application of 2D NMR correlation information in computer-assisted structure elucidation of complex natural products. *J Chem Inf Comput Sci* 34(4):805–813
81. Peng C, Yuan S, Zheng J (1995) Practical computer-assisted structure elucidation for complex natural products: efficient use of ambiguous 2D NMR correlation information. *J Chem Inf Comput Sci* 35(3):539–546

82. Pirkle WH, Beare SD (1967) Nonequivalence of the nuclear magnetic resonance spectra of enantiomers in optically active solvents. IV. Assignment of absolute configuration. *J Am Chem Soc* 89(21):5485–5487
83. Randall EW (1997)  $^1\text{H}$  and  $^{19}\text{F}$  magnetic resonance imaging of solid paramagnetic compounds using large magnetic field gradients and Hahn echoes. *Solid State Nucl Magn Reson* 8(3):173–178
84. Reynolds WF, Yu M, Enriquez RG, Leon I (1997) Investigation of the advantages and limitations of forward linear prediction for processing 2D data sets. *Magn Reson Chem* 35(8):505–519
85. Rinaldi PL (1983) Heteronuclear 2D-NOE spectroscopy. *J Am Chem Soc* 105(15):5167–5168
86. Roberts GCK (2000) Applications of NMR in drug discovery. *Drug Discovery Today* 5:230–240
87. Russell DJ, Hadden CE, Martin GE, Gibson AA, Zens AP, Carolan JL (2000) *J Nat Prod* 63(8):1047–1049
88. Rüdiger A-H, Rüdiger M, Carl UD, Chakraborty T, Roepstorff P, Wehland J (1999) Affinity mass spectrometry approaches for the analysis of protein-protein interaction and complex mixtures of peptides. *Anal Biochem* 275:162–170
89. Sanders JKM, Hunter BK (1993) *Modern NMR spectroscopy: a guide for chemists*. Oxford University Press
90. Scarfe GB, Clayton E, Wilson ID, Nicholson JK (2000) Identification and quantification of metabolites of 2,3,5,6-tetrafluoro-4-trifluoromethylaniline in rat urine using fluorine-19 nuclear magnetic resonance spectroscopy, high-performance liquid chromatography-nuclear magnetic resonance spectroscopy and, high-performance liquid chromatography-mass spectrometry. *J Chromatogr B Biomed Appl* 748(1):311–319
91. Schriber H, Pretsch E (1997) General characterisation of good-list and bad-list entries for structure generators from spectra. *J Chem Inf Comput Sci* 37:879–883
92. ScienceSoft, LLC, Salt Lake City, Utah USA NMRanalyst/FRED <http://www.sciencesoft.net/index.html>
93. Serre AM, Roby C, Roscher A, Nurit F, Euvrard M, Tissut M (1997) Comparative detection of fluorinated xenobiotics and their metabolites through  $^{19}\text{F}$  NMR or  $^{14}\text{C}$  label in plant cells. *J Agric Food Chem* 45:242–248
94. Shapiro MJ, Kumaravel G, Petteer RC, Beveridge R (1996)  $^{19}\text{F}$  NMR monitoring of an  $\text{S}_{\text{N}}\text{Ar}$  reaction on solid support. *Tetrahedron Lett* 37(27):4671–4674
95. Shapiro MJ, Wareing JR (1998) NMR methods in combinatorial chemistry. *Curr Opin Chem Biol* 2:372–375
96. Shuker SB, Hajduk PJ, Meadows RP, Fesik SW (1996) Discovering high-affinity ligands for proteins: SAR by NMR. *Science* 274:1531–1534
97. Sidelmann UG, Nicholls AW, Meadows PE, Gilbert JW, Lindon JC, Wilson ID, Nicholson JK (1996) High-performance liquid chromatography directly coupled to  $^{19}\text{F}$  and  $^1\text{H}$  NMR for the analysis of mixtures of isomeric ester glucuronide conjugates of trifluoromethylbenzoic acids. *J Chromatogr A* 728:377–385
98. Smallcombe SH, Patt SL, Keifer PA (1995) WET solvent suppression and its application to LC NMR and high-resolution spectroscopy. *J Magn Reson Ser A* 117(2):295–303
99. Spectrum Research, LLC, Madison, Wisconsin USA <http://www.specres.com/nmrsams.asp>
100. Spraul M, Hofmann M, Wilson ID, Lenz E, Nicholson JK (1993) Coupling of HPLC with  $^{19}\text{F}$  and  $^1\text{H}$ -NMR spectroscopy to investigate the human urinary excretion of flurbiprofen metabolites. *J Pharm Biomed Anal* 11(10):1009–1015
101. Stockman BJ (1998) NMR spectroscopy as a tool for structure based design. *Prog Nucl Magn Reson Spectrosc* 33(2):109–151
102. Stott K, Keeler J (1996) Gradient-enhanced one-dimensional heteronuclear NOE experiments with  $^1\text{H}$  detection. *Magn Reson Chem* 34(7):554–558
103. Sweatman BC, Farrant RD, Holmes E, Ghuari FYK, Nicholson JK, Lindon JC (1993) 600 MHz proton-NMR spectroscopy of human cerebrospinal fluid: effects of sample manipulation and assignment of resonances. *J Pharm Biomed Anal* 11(8):651–664

104. Svensson A, Fex T, Kihlberg J (1996) Use of  $^{19}\text{F}$  NMR spectroscopy to evaluate reactions in solid phase organic synthesis. *Tetrahedron Lett* 37 (42):7649–7652
105. Uhrin D, Beatty EJ, Sandór P, McSparron S, Wilken J, Starkmann B, Young DW, Barlow PN, Ramage R (1999)  $^{19}\text{F}$ - $^1\text{H}$  Correlation at no extra cost. *Magn Moments* 10(1):9–15
106. Vikić-Topić D, Meić Z (1986) Carbon-fluorine long range coupling for estimating molecular conformations. *J Mol Struct*: 142–148
107. Wagner R, Berger S (1996) Gradient-selected NOESY – a fourfold reduction of the measurement time for NOESY experiments. *J Magn Reson Ser A* 123(1):119–121
108. Warne MA, Lenz EM, Osborn D, Weeks JM, Nicholson JK (2000) An NMR-based metabonomic investigation of the toxic effects of 3-trifluoromethylaniline on the earthworm *Eisenia venata*. *Biomarkers* 5(1):56–72
109. Willoughby R, Sheehan E, Mitrovich S (1998) A global view of LC/MS – how to solve your most challenging analytical problems. Global View Publishing
110. Wilson ID, Nicholson JK (1987) Solid-phase extraction chromatography and nuclear magnetic resonance spectrometry for the identification and isolation of drug metabolites in urine. *Anal Chem* 59(23):2830–2832
111. Wray V (1980) *Annu Rep NMR Spectrosc* 10B:1
112. Wray V (1983) *Annu Rep NMR Spectrosc* 14:1
113. Zhou L, Rajabzadeh M, Traficante D, Cho BP (1997) Conformational heterogeneity of arylamine-modified DNA:  $^{19}\text{F}$  NMR evidence. *J Am Chem Soc* 119(23):5384–5389